Development/Plasticity/Repair

5-HT_7R/G_{12} Signaling Regulates Neuronal Morphology and Function in an Age-Dependent Manner

Fritz Kobe,[1,2]* Daria Guseva,[3]* Thomas P. Jensen,[4]* Alexander Wirth,[3] Ute Renner,[1,2] Dietmar Hess,[1,2] Michael Müller,[1,2] Lucian Medrihan,[1,2] Weiqi Zhang,[1,5] Mingyue Zhang,[5] Katharina Braun,[6] Sören Westerholz,[6] Andreas Herzog,[7] Konstantin Radyushkin,[8] Ahmed El-Kordi,[8] Hannelore Ehrenreich,[8] Diethelm W. Richter,[1,2] Dmitri A. Rusakov,[4] and Evgeni Ponimaskin[1,3]

[1]DFG-Research Center Molecular Physiology of the Brain (CMPB) and [2]Department of Neuro- and Sensory Physiology, University of Göttingen, 37073 Göttingen, Germany, [3]Cellular Neurophysiology, Center of Physiology, Medical School Hannover, 30625 Hannover, Germany, [4]Institute of Neurology, University College London, London, United Kingdom, [5]Laboratory of Molecular Psychiatry, Department of Psychiatry, University of Münster, 48149 Münster, Germany, [6]Department of Zoology/Developmental Neurobiology and [7]Institute for Electronics, Signal Processing and Communications, Otto-von-Guericke-University Magdeburg, 39120 Magdeburg, Germany, and [8]Max-Planck-Institute of Experimental Medicine, 37075 Göttingen, Germany

The common neurotransmitter serotonin controls different aspects of early neuronal differentiation, although the underlying mechanisms are poorly understood. Here we report that activation of the serotonin 5-HT_7 receptor promotes synaptogenesis and enhances synaptic activity in hippocampal neurons at early postnatal stages. An analysis of $G\alpha_{12}$-deficient mice reveals a critical role of G_{12}-protein for 5-HT_7 receptor-mediated effects in neurons. In organotypic preparations from the hippocampus of juvenile mice, stimulation of 5-HT_7R/G_{12} signaling potentiates formation of dendritic spines, increases neuronal excitability, and modulates synaptic plasticity. In contrast, in older neuronal preparations, morphogenetic and synaptogenic effects of 5-HT_7/G_{12} signaling are abolished. Moreover, inhibition of 5-HT_7 receptor had no effect on synaptic plasticity in hippocampus of adult animals. Expression analysis reveals that the production of 5-HT_7 and $G\alpha_{12}$-proteins in the hippocampus undergoes strong regulation with a pronounced transient increase during early postnatal stages. Thus, regulated expression of 5-HT_7 receptor and $G\alpha_{12}$-protein may represent a molecular mechanism by which serotonin specifically modulates formation of initial neuronal networks during early postnatal development.

Introduction

Serotonin [5-hydroxytryptamine (5-HT)] is an important neurotransmitter regulating a wide range of physiological and pathological functions via activation of heterogeneously expressed 5-HT receptors (Olson, 1987; Hilaire et al., 1993; Saito et al., 1999; Naughton et al., 2000; Narita et al., 2001; Woehler and Ponimaskin, 2009). In addition to its well established role in the modulation of neuronal communication, serotonin has been shown to be involved in many aspects of neural development, such as neurite outgrowth, regulation of somatic morphology, growth cone motility, and control of dendritic spine shape and density (Azmitia, 2001; Kvachnina et al., 2005; Udo et al., 2005; Ponimaskin et al., 2007; Manzke et al., 2009). It also has been shown that morphogenic effects of serotonin undergo developmental regulation and, more importantly, that availability of serotonin during sensitive developmental stages can modulate formation and functions of behaviorally relevant neuronal networks in adulthood (Herlenius and Lagercrantz, 2001; Whitaker-Azmitia, 2005). Although several serotonin receptors, including 5-HT_{1A}, 5-HT_2, and 5-HT_4, have been proposed to modulate morphogenic events elicited by 5-HT (Yan et al., 1997; Fiorica-Howells et al., 2000; Azmitia, 2001), the underlying molecular mechanisms, in particular those involved in developmental regulation, remain poorly understood.

We have recently found that the serotonin receptor 5-HT_7 is coupled to the heterotrimeric G_{12}-protein, which in turn selectively activates small GTPases RhoA and Cdc42 (Kvachnina et al., 2005). Multiple studies suggest that Cdc42 is a positive regulator promoting neurite outgrowth, spine structural plasticity, and growth cone protrusion. Conversely, activation of RhoA induces stress fiber formation, leading to growth cone collapse and neurite retraction (Lee et al., 2000; Li et al., 2000; Newey et al., 2005). In accordance with these observations, we have demonstrated that agonist-dependent activation of the 5-HT_7 receptor in neuroblastoma cells induced pronounced filopodia formation via a Cdc42-mediated pathway paralleled by RhoA-dependent cell rounding. Moreover, stimulation of endogenous 5-HT_7 receptors in hippocampal neurons resulted in a marked elongation of neurites (Kvachnina et al., 2005).

Received June 3, 2011; revised Dec. 28, 2011; accepted Dec. 31, 2011.

Author contributions: W.Z., K.B., K.R., A.E.-K., H.E., D.W.R., D.A.R., and E.P. designed research; F.K., D.G., T.P.J., A.W., U.R., D.H., M.M., L.M., M.Z., S.W., K.R., A.E.-K., and E.P. performed research; F.K., D.G., T.P.J., A.W., U.R., D.H., M.M., L.M., W.Z., M.Z., K.B., S.W., A.H., K.R., A.E.-K., H.E., D.A.R., and E.P. analyzed data; F.K., D.G., D.W.R., D.A.R., and E.P. wrote the paper.

*F.K., D.G. and T.P.J. contributed equally to this work.

The authors declare no competing financial interests.

These studies were supported by Deutsche Forschungsgemeinschaft Grants PO732 and SFB621/C12 (E.G.P.) and by the Center of Molecular Physiology of the Brain, the Wellcome Trust, and MRC UK. We are very grateful to Dr. David R. Thomas (GlaxoSmithKline, Harlow, UK), who kindly provided us with the 5-HT_7 antagonist SB656104-A.

Correspondence should be addressed to Evgeni Ponimaskin, Department of Cellular Neurophysiology, Carl-Neuberg-Strasse 1, 30625 Hannover, Germany. E-mail: Ponimaskin.Evgeni@mh-hannover.de.

DOI:10.1523/JNEUROSCI.2765-11.2012

 0270-6474/12/322915-16$15.00/0

In the present study, we found that activation of the 5-HT$_7$R/G$_{12}$ signaling pathway promotes formation of dendritic protrusions and synaptogenesis in cultured hippocampal neurons, leading to enhanced spontaneous synaptic activity. In organotypic hippocampal cultures from juvenile mice, 5-HT$_7$R/G$_{12}$ signaling potentiates formation of dendritic spines, increases the basal neuronal excitability, and modulates synaptic plasticity. Although prominent in juvenile mice, the effects of the 5-HT$_7$R/G$_{12}$ signaling on synaptic plasticity are abolished in adult animals. This dichotomy in the efficacy of 5-HT$_7$R/G$_{12}$ signaling between juvenile and adult animals is consistent with a decrease in the hippocampal expression of both 5-HT$_7$ and Gα_{12}-proteins during later development. Our results suggest that the tightly regulated expression of the 5-HT$_7$ receptor and the Gα_{12}-protein represents a molecular mechanism involved in the serotonin-mediated regulation of neuronal morphology and function during early development.

Materials and Methods

Culturing and transfection of hippocampal neurons. Hippocampal cultures were prepared from postnatal day 1 (P1) or P2 National Maritime Research Institute (NMRI) mice according to an optimized protocol for mouse hippocampal neurons (Dityatev et al., 2000). Briefly, hippocampi were isolated, and dissociated neurons were plated at a density of 25–30 $\times$ 10^3 cells per coverslip onto sterilized 13 mm coverslips coated with poly-L-lysine (100 μg/ml) and laminin (40 μg/ml). During the first 3 d, cells were incubated in culture medium [MEM Eagle's medium containing glucose (25.2 mM), transferrin (1.3 mM), insulin (25 μg/ml), Glutamax I (2 mM), gentamicin (0.5 μl/ml), and horse serum (0.1 ml/ml)] at 37°C and 5% CO$_2$. On the fourth day *in vitro* (DIV4), the medium was replaced by Neurobasal-A medium containing L-glutamine (0.5 mM), b-FGF (125 ng/ml), B-27 supplement (20 μl/ml), penicillin/streptomycin (10 μl/ml), and cytosine arabinoide (5 μM) to feed the cell cultures and to prevent glial mitosis.

Organotypic hippocampal slice cultures were prepared according to the method described for rats (Stoppini et al., 1991) after adaptation for mice. In brief, hippocampi from P6 NMRI mice were isolated and cut in slices of 350 μm thickness. These slices were then maintained on a biomembrane surface (0.4 μm, Millicell-CM; Millipore) in culture medium (50% MEM, 25% Hanks' balanced salt solution, 25% horse serum, and 2 mM glutamine at pH 7.3) under a humidified atmosphere (5% CO$_2$, 36.5°C). The slices were used for experiments after 7–10 d *in vitro* incubation. All animals were housed, cared for, and killed in accordance with the recommendations of the European Commission.

For morphological analysis, neurons were transfected at DIV4 (dissociated neurons) and at DIV2 (organotypic preparations) with 1 μg of pcDNA3.1 vector encoding GFP by using Lipofectamine2000 reagent (Invitrogen). For the knock-down experiments, hippocampal neurons on DIV7 were transfected with pSUPER/GFP short interfering RNA (siRNA) expression plasmid (Oligoengine) targeting the 5-HT$_7$ receptor. Agonist/antagonist treatment was started at DIV8, followed by the morphological analysis at DIV12. Two different siRNA plasmids for specific knockdown of 5-HT$_7$ receptors were constructed by the cloning of 60 bp double-stranded oligonucleotides containing a 19 bp target sequence into the pSUPER/GFP vector between the BglII and HindIII sites. The 19 bp target sequences for these selected siRNA constructs were 5′-TTCT CTCTGCCTCCATCAC-3′ and 5′-TCCATCACCTTACCTCCTC-3′. The "target" for the scrambled siRNA control construct was 5′-AGAC TCTTTCTTGCTTGT-3′. For the knock-down experiments, hippocampal neurons at DIV7 were transfected either with the mix of two pSUPER/GFP expression plasmids encoding for 5-HT$_7$ receptor siRNAs or with the vector containing scramble siRNA by using Lipofectamine2000. Expression vectors also contained GFP, allowing for simple identification of transfected neurons by green fluorescence.

Immunocytochemistry and dendrite morphology analysis. For immunocytochemistry, primary antibodies were used at the following concentrations: goat polyclonal anti-synaptophysin (1:50; Santa Cruz Biotechnology), rabbit polyclonal anti-PSD-95 (1:200; Santa Cruz Biotechnology), mouse monoclonal anti-PSD-95 (1:500; Millipore), rabbit polyclonal anti-5-HT$_7$ receptor (1:500; AbD Serotec), goat polyclonal anti-Gα_{12} (1:100; Santa Cruz Biotechnology), rabbit polyclonal anti-Gα_{12} (1:500; Kvachnina et al., 2005), rat monoclonal anti-5-HT (1:100; Santa Cruz Biotechnology), rabbit polyclonal anti-AMPA receptor (AMPAR; 1:500; Abcam), and rabbit polyclonal anti-vesicular GABA transporter (VGAT; 1:500, Synaptic Systems).

For the analysis of dendritic morphology, images of GFP-transfected neurons were acquired under a Zeiss LSM510-Meta laser-scanning confocal microscope with a 40$\times$ oil-immersion Plan-Neofluor objective. Dendritic filopodia with a length of 10–30 μm were evaluated as long protrusions (LPs) and those shorter than 10 μm as short protrusions (SP). To analyze the number of synaptic clusters, synaptophysin-positive puncta were calculated along the dendrite of GFP-transfected neurons. At least 30 randomly collected images were used for each treatment protocol, and the number of synaptophysin-positive puncta was calculated per 50 μm of the entire dendritic length.

Analysis of dendritic spine morphology in organotypic cultures was performed after collecting *z*-stack images of individual neurons transfected with GFP. Three-dimensional reconstruction was performed by using self-developed software (Herzog et al., 2006), which enables measurement of the full geometric parameters of dendritic spines (i.e., number, length, size, volume, surface area).

Retrograde labeling of floating sections and spine density analysis. Analysis of the neuronal fine structure in wild-type and Gα_{12}-deficient mice was performed in acute hippocampal slices after visualization of CA1 pyramidal neurons by 1,1′-dioctadecyl-3,3,3′,3′-tetramethylindocarbocyanine perchlorate (DiI) crystals, according to the protocol described by Morita et al. (2009).

Analysis of 5-HT$_7$ receptor and 5-HT distribution. For the analysis of 5-HT$_7$ receptor and 5-HT distribution in hippocampus during development, 10-μm-thick hippocampal cryosections prepared from mice at P2, P6, and P90 were subjected to immunohistochemistry followed by confocal microscope analysis by using an FV1000 microscope (Olympus) with a 60$\times$ oil-immersion objective. Briefly, after incubation with primary antibodies, appropriate Alexa-546-, Alexa-488-, DyLight488-, DyLight549-, and DyLight649-conjugated secondary antibodies (Jackson ImmunoResearch Laboratories) were applied at the dilution of 1:400. Cell nuclei were stained with *bis*-benzimide solution (Hoechst 33258 dye, 5 μg/ml in PBS; Sigma-Aldrich), and the sections were mounted in antiquenching medium (Fluoromount G; Southern Biotechnology Associates). Stacks of optical sections of 0.3 μm thickness were used to estimate colocalization of 5-HT and 5-HT$_7$ receptor-positive puncta in the CA1 area of hippocampus. At least 10 neurons per hippocampus were counted ($n = 30$). Statistical analysis of the integrated intensity plot profiles was analyzed using Student's *t* test.

Immunohistochemistry and analysis of AMPA receptors and synaptophysin expression. To compare the level of AMPARs and VGAT in control and 5-CT-treated organotypic slices from the mouse hippocampus, we used immunohistochemistry for floating sections. Briefly, organotypic slices were removed from the biomembrane surface and fixed with 4% formaldehyde in 0.1 M sodium cacodylate buffer, pH 7.3. Blocking of nonspecific binding sites was performed using PBS containing 0.2% Triton X-100 (Sigma-Aldrich), 0.02% sodium azide (Merck), and 5% donkey serum (Jackson ImmunoResearch Laboratories) for 1 h at room temperature. Incubation with primary antibodies against synaptophysin, VGAT, and AMPARs [all diluted in PBS containing 0.5% lambda-carrageenan (Sigma-Aldrich) and 0.02% sodium azide] was performed at 4°C for 3 d. After washing in PBS, corresponding secondary antibodies (Jackson ImmunoResearch Europe) diluted 1:200 in PBS–carrageenan solution were applied for 2 h at room temperature. Quantitative immunofluorescence analysis was performed according to the method recently described by Chao et al. (2007). Briefly, all images were acquired and analyzed blinded to treatment on a Zeiss 510 laser-scanning confocal microscope with settings to allow the pixel intensities to remain within the dynamic range by using a 10$\times$ objective and digital resolution of 2048 $\times$ 2048 pixels. Fluorescence intensity for synaptophysin, VGAT, and AMPARs was analyzed by using ImageJ software (http://rsb.info.nih.gov/ij/) after subtraction of back-

ground. Statistical analysis of the integrated intensity plot profiles was analyzed using Student's *t* test.

Electrophysiological recordings. Whole-cell patch-clamp recordings from dissociated hippocampal neuronal cultures at DIV11 were performed in the current-clamp mode with a patch-clamp amplifier EPC-9 using Pulse software (HEKA). The extracellular solution contained (in mM) 118 NaCl, 2 KCl, 10 glucose, 10 HEPES, 2 $CaCl_2$, and 1 $MgCl_2$, pH 7.4. Patch electrodes were filled with the intracellular solution composed of (in mM) 1 NaCl, 125 K-gluconate, 10 HEPES, 0.5 $CaCl_2$, 1 $MgCl_2$, 11 EGTA, 1 ATP, and 0.3 GTP, with a pH adjusted to 7.4. The recordings were filtered at 10 kHz (four-pole Bessel filter), and the frequency of single EPSPs and action potentials were measured each second. All electrophysiological data were transferred to a PC-readable format and analyzed by Clampfit 8 (Molecular Devices) and PlotIT (Scientific Programming Enterprises). Values of the individual parameters are presented as mean ± SEM, with *n* giving the number of recorded neurons. Significance of effects was determined by two-tailed unpaired Student's *t* tests.

For the analysis of long-term potentiation (LTP) in organotypic preparations, single slices were constantly perfused in an interface recording chamber (Oslo type) with the ACSF containing (in mM) 130 NaCl, 3.5 KCl, 1.25 NaH_2PO_4, 24 $NaHCO_3$, 1.2 $CaCl_2$, 1.2 $MgSO_4$, and 10 dextrose, aerated with 95% O_2 and 5% CO_2, pH to 7.4. The temperature was adjusted to 31–32°C. The field EPSPs (fEPSPs) were evoked orthodromically, by a stimulation electrode placed in the stratum radiatum at the CA3/CA1 junction to activate Schaffer collateral axons. The recording electrode was placed in the stratum radiatum of the CA1 region. The magnitude of fEPSPs was measured as amplitude (baseline to peak) and slope (20–80% level of the falling phase). For input–output (IO) relationships, fEPSPs were evoked with 0.1 ms stimuli at 0.25 Hz, and an average of four consecutive responses was taken. fEPSP amplitudes and slopes were plotted against the stimulus intensity (10–150 μA). Paired-pulse facilitation (PPF) was measured as the ratio of the second fEPSP to the first fEPSP evoked at different interstimulus intervals (25, 50, 75, 100, 125, 150, 175, and 200 ms). The paired stimuli were set at 0.25 Hz, and an average of four consecutive responses was obtained. For LTP, baseline responses were evoked every 20 s for 5 min, and LTP was induced by one train consisting of 100 Hz stimulation for 1 s. The posttrain responses were then measured every 20 s for 60 min, and an average of four consecutive responses was taken. For PPF and LTP recordings, stimulation intensity was adjusted to obtain ~50% response magnitudes. Evoked responses were elicited by 0.1 ms unipolar stimuli (Grass S88 stimulator with PSIU6 photoelectric stimulus isolation units; Grass Instruments) delivered via microwire electrodes made from bare stainless steel wire (50 μm diameter; A-M Systems) and recorded as described previously (Müller and Somjen, 1998). Responses were recorded using a locally constructed extracellular DC potential amplifier and digitized by a DigiData 1322A (Molecular Devices). Data analysis was performed in Clampfit 9.0 (Molecular Devices).

Experiments in acute hippocampal slices were performed on the C57BL/6NCrl (Charles River Laboratories) mouse strain. Mice were housed at four to five per cage in a room with a 12 h light/dark cycle (lights on at 8:00 A.M.) and had *ad libitum* access to food/water. Experiments were permitted by the local Animal Care and Use Committee. The 5-HT$_7$ receptor antagonist SB656104-A, which was kindly provided by Dr. D. R. Thomas (GlaxoSmithKline, Harlow, UK), was dissolved in 10% Captisol/saline solution (Cydex) and administered intraperitoneally at the dose 20 mg/kg twice per day (8:00 A.M. and 8:00 P.M.) for 3 weeks. Freshly made solution was used each day. The volume of injection was 0.01 ml/g of mouse body weight. Control animals were identically treated with the corresponding volume of 10% Captisol/saline vehicle solution.

Two-photon excitation Ca^{2+} imaging in hippocampal slices. Acute 300 μm hippocampal slices were prepared from P12–P16 male C57/BL6 mice using techniques described previously (Kochlamazashvili et al., 2010). To examine postsynaptic Ca^{2+} entry induced by backpropagating action potentials, slices were transferred to a submersion-type recording chamber (Scientific Systems Design) and superfused with (in mM) 124 NaCl, 2.5 KCl, 2 $CaCl_2$, 1.3 $MgSO_4$, 26 $NaHCO_3$, and 10 glucose bubbled with 95% O_2/5% CO_2 at 32°C. The internal solution contained (in mM) 135 K methanesulfonate, 2 $MgCl_2$, 10 HEPES, 10 tris-phosphocreatine, 4 NaATP, 0.4 NaGTP, 0.05 Alexa Fluor 594 hydrazide sodium salt (Invitrogen), and 0.4 Fluo-4 pentapotassium salt (Invitrogen). In all recordings, 10 μM NBQX, 50 μM APV, and 100 μM picrotoxin were added to the extracellular solution to block synaptic transmission.

Imaging experiments were performed using a Radiance 2100 imaging system (Zeiss-Bio-Rad) linked to a femtosecond pulse laser MaiTai (SpectraPhysics-Newport) and integrated with patch-clamp electrophysiology (Rusakov and Fine, 2003). CA1 pyramidal cells were held in voltage clamp at −70 mV, and dye equilibration was allowed for 20–25 min before recording started. Backpropagating action potentials were induced by 3 ms command voltage pulses. Fluo-4 and Alexa fluorescence was chromatically separated and collected by line scanning at 500 Hz. Four to six scans of an individual spine or dendrite were averaged for analyses. The background-corrected Ca^{2+}-dependent fluorescent signal in the "green" Fluo-4 channel (G) was normalized to the "red" Alexa 594 channel fluorescence (R) to account for focus fluctuations. In each experiment, the average Ca^{2+}-sensitive signal was calculated as the total Ca^{2+}-dependent fluorescence integrated over the recording time normalized against R, $\Delta G/R$.

To document Ca^{2+} responses evoked in individual postsynaptic dendritic spines of CA1 pyramidal cells by synaptic activation (optical quantal analysis), the cell was filled with the internal solution described previously, and with the inclusion of 5 mM QX-314, 50 μM Alexa Fluor 594, and 400 μM Fluo-4 was held at $V_m = -60$ mV in the presence of 100 μM picrotoxin and 30 μM D-serine. The recording procedure followed the previously described routines (Oertner et al., 2002; Emptage et al., 2003). A monopolar glass stimulating electrode (patch pipette) filled with ACSF was placed 15–30 μm from the dendritic branch targeted. To identify active synapses, relatively fast (10 Hz) frame scans of the local dendrites were viewed while three 100 μs square pulses of 2–10 V were delivered with a 25 ms interstimulus interval using a constant voltage isolated stimulator (model DS2A-mkII; Digitimer Ltd.). This protocol was repeated until a Ca^{2+} response confined to a spine head was observed, and 400–500 ms line scans (positioned across the head of an active spine) were then recorded while a pair of stimuli (50 ms interstimulus interval) was delivered. Scans were repeated once every 30 s with a minimum of 15 trials in each condition to assess release probability at the imaged synapse. Failures and successes of postsynaptic Ca^{2+} transients were clearly distinguishable in each trial (experiments in which the signal-to-noise ratio was <3 were discarded).

Real-time quantitative RT-PCR analysis. The total RNA from the hippocampus of mice at different postnatal ages was isolated using TRIzol Reagent (Invitrogen) in conjunction with PureLink Micro-to-Midi Total RNA Purification System (Invitrogen). The expression analysis was performed on a ABI PRISM7000 Sequence Detector (Applied Biosystems) using TaqMan Universal PCR Master Mix (Applied Biosystems). For the detection of 5-HT$_7$, 5-HT$_4$, Gα_S, and Gα_{12} mRNA, corresponding Gene Expression Assays (Applied Biosystems) containing gene-specific primers were used. For quantitative analysis, eukaryotic 18S RNA was analyzed in parallel. The analysis was performed by using delta-delta-C_t method according to the procedure described at http://www3.appliedbiosystems.com/AB_Home/index.htm.

Results

5-HT$_7$ receptor stimulation induces formation of dendritic protrusions and synaptogenesis

We have recently found that the 5-HT$_7$ receptor is functionally coupled to the heterotrimeric G$_{12}$-proteins and that its stimulation results in G$_{12}$-mediated activation of the small GTPase Cdc42, leading to neurite outgrowth (Kvachnina et al., 2005). To investigate the role of the 5-HT$_7$R/G$_{12}$ signaling pathway in dendritic morphogenesis, we used primary cultures of hippocampal neurons, which allowed for visualization of the morphological changes and for functional analysis. We selected a time window from DIV10 to DIV12, when well defined synapses are already formed (Bartrup et al., 1997; Fig. 1*F*). To monitor receptor-mediated morphological changes, GFP-transfected neurons were

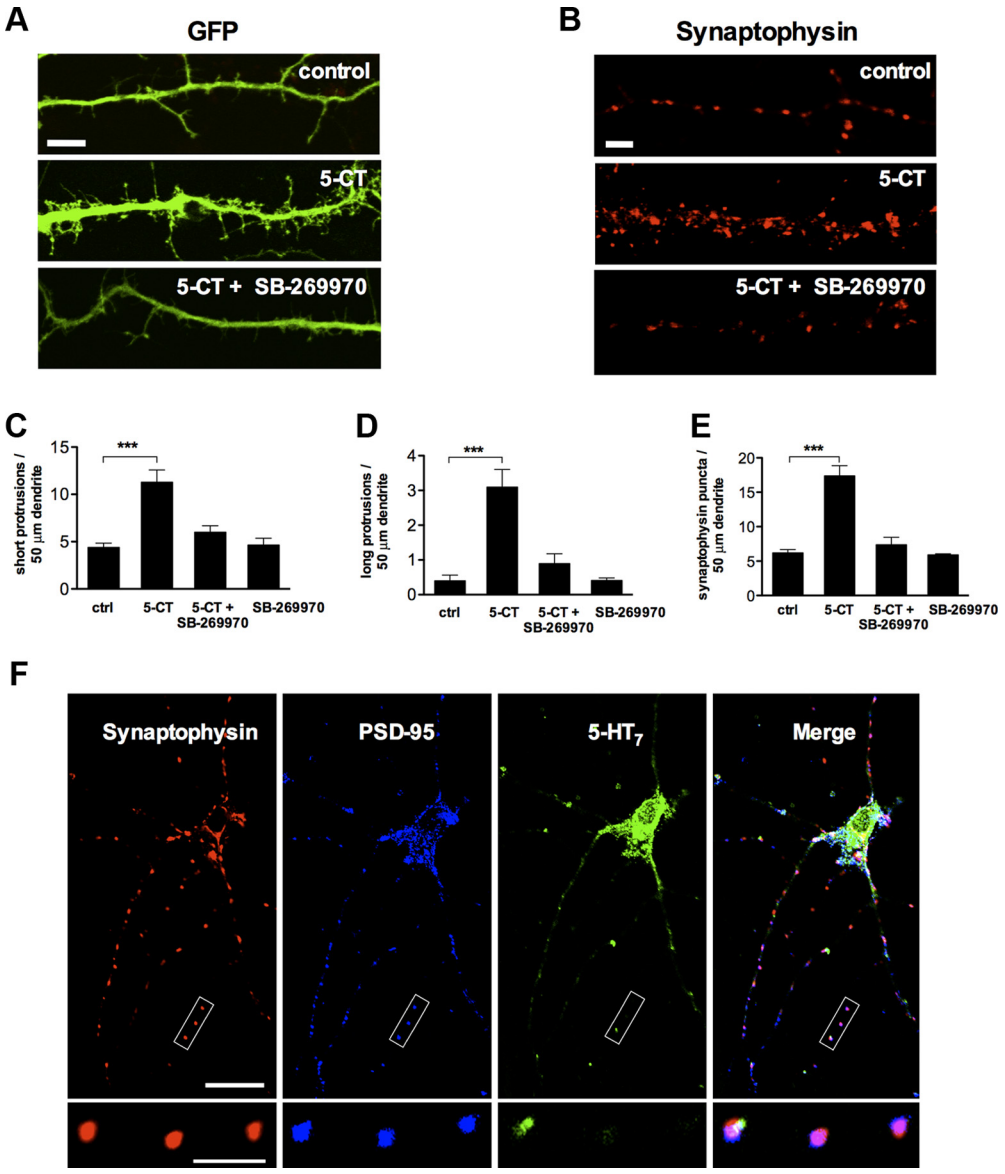

Figure 1. Stimulation of the 5-HT$_7$ receptor induces formation of dendritic filopodia and synaptic clusters. ***A***, Representative image showing dendritic morphology of control (top), 5-CT (100 nM; middle), and 5-CT (100 nM) plus SB-269970 (1 μM; bottom) treated neurons. Scale bar, 10 μm. ***B***, Synaptophysin puncta in dendrites of control (top), 5-CT (100 nM; middle), and 5-CT (100 nM) plus SB-269970 (1 μM; bottom) treated neurons. Scale bar, 10 μm. ***C***, ***D***, The number of short (*C*; <10 μm) and long (***D***; >10 μm) dendritic protrusions is significantly increased in 5-CT-treated neurons compared with the control (ctrl) neurons. The morphogenic effect is receptor specific because it is inhibited by SB-269970, an antagonist of the 5-HT$_7$ receptor. Values represent mean $\pm$ SEM; ***$p < 0.001$ ($n = 30$). ***E***, Quantification of synaptophysin-positive puncta in control (ctrl) and in 5-CT-treated neurons. The synaptogenic effect of 5-CT is abolished after treatment with the 5-HT$_7$ receptor antagonist SB-269970. The number of dendritic protrusions and synaptophysin-positive puncta are calculated per 50 μm of dendrite. Values represent means $\pm$ SEM; ***$p < 0.001$ ($n = 30$). ***F***, Confocal microscope image of untreated hippocampal neurons at DIV11. The synapses formed in cultured neurons appear to be structurally intact, as defined by the colocalization of the postsynaptic density protein PSD-95 and synaptophysin puncta. Expression of the 5-HT$_7$ receptor was observed both in cell body and dendrites. The bottom high-magnification images represent a part of the neurite where the 5-HT$_7$ receptor is colocalized with presynaptic (synaptophysin) and postsynaptic (PSD-95) markers. Scale bars: top, 20 μm; bottom, 10 μm.

incubated with a low concentration of the 5-HT$_7$ receptor agonist 5-CT (100 nM) during the last 4 d before analysis.

Agonist treatment substantially increased the number of dendritic protrusions compared with nontreated controls (Fig. 1*A*, *C*, *D*). The number of SPs per 50 μm of dendritic length was 4.4 $\pm$ 0.45 in control versus 11.3 $\pm$ 1.27 after 5-CT treatment (Fig. 1*C*; $n = 30$; $p < 0.001$), and the number of LPs (over 10 μm) was 0.4 $\pm$ 0.16 in control versus 3.1 $\pm$ 0.5 after 5-CT treatment (Fig. 1*D*; $n = 30$; $p < 0.001$). These morphogenic effects were receptor specific because they were inhibited by the antagonist of the 5-HT$_7$ receptor, SB-269970 (Fig. 1*C*,*D*). It is noteworthy that treatment of neurons with antagonist alone does not result in any significant morphological changes when compared with the control (SP, 4.6 $\pm$ 0.71; LP, 0.4 $\pm$ 0.07; $n = 10$; Fig. 1*C*,*D*).

To determine whether the 5-HT$_7$ receptor-mediated signaling affects synaptic density, we quantified the number of synapses by labeling GFP-transfected neurons with the presynaptic marker synaptophysin (De Paola et al., 2003; Fig. 1*B*). Treatment of neurons with 5-CT increased the number of synaptophysin-positive puncta from 6.2 $\pm$ 0.49 to 17.4 $\pm$ 1.46 ($n = 30$; $p < 0.001$) per 50 μm of dendrite (Fig. 1*E*). Similarly to the effects on the formation of dendritic protrusions, the synaptogenic effect of 5-CT was abolished by the 5-HT$_7$ receptor antagonist (Fig. 1*E*). The synapses formed in both 5-CT-treated and control neurons appear

to be structurally intact, as defined by the tight colocalization of the postsynaptic density protein PSD-95 and synaptophysin-positive puncta (99.4 ± 0.4 and 98.8 ± 1.3% of PSD-95 puncta was colocalized with synaptophysin in untreated and 5-CT-treated cultures, respectively. Accordingly, 97.7 ± 0.9 and 98.8 ± 1.3% of synaptophysin puncta were colocalized with PSD-95). A small fraction of the 5-HT$_7$ receptor (9.5 ± 2.1%) was colocalized with presynaptic and postsynaptic markers in neurons, suggesting that 5-HT$_7$ receptor-mediated signal transduction can occur within close proximity of the synapse (Fig. 1*F*). Notably, the receptor distribution was not changed after 5-CT treatment.

Morphogenic and synaptogenic effects of the 5-HT$_7$ receptor are mediated by the Gα_{12}-protein

In addition to coupling to the heterotrimeric G$_{12}$-protein, the 5-HT$_7$ receptor can stimulate cAMP formation by activating adenylyl cyclases via a stimulatory G$_s$-protein. The G$_s$-mediated signaling in turn can regulate the cellular morphology either by modulating cAMP concentration (Iyengar, 1996; Corset et al., 2000) or by direct binding of Gα_s to the cytoskeleton (Yu et al., 2009). To investigate whether the morphogenic effects of the 5-HT$_7$ receptor include the G$_s$-mediated component, we analyzed primary hippocampal neurons prepared from Gα_{12}-deficient mice. Initial studies in the Gα_{12}-knock-out mouse have found no apparent phenotype (Gu et al., 2002). An analysis of dendritic morphology revealed that, without any treatment, the number of dendritic protrusions in Gα_{12}-knock-out neurons was significantly reduced compared with wild type (SP, to 72.5 ± 3.7%; LP, to 68. 2 ± 11.8%; relative to wild type; $n = 30$; $p < 0.001$; Fig. 2*B*,*C*). In addition, the density of synapses assessed by the analysis of synaptophysin-positive puncta was reduced to 88.5 ± 3.2% relative to wild type ($n = 30$; $p < 0.001$; Fig. 2*D*), suggesting that basal Gα_{12}-mediated activity is involved in morphogenesis and synapse formation. A statistical analysis performed on neurons isolated from Gα_{12}-deficient mice revealed that both the number of dendritic protrusions and the density of synaptophysin-positive puncta were indistinguishable between 5-HT$_7$ receptor agonist treated and nontreated neurons (5-CT: SP, 81 ± 5.9%; LP, 65.9 ± 10.6%; synaptic cluster density, 86.9 ± 2.9%; Fig. 2*B*,*C*). In contrast, these parameters were significantly increased after agonist treatment of neurons prepared from the wild-type animals (5-CT: SP, 169 ± 10%; LP, 245 ± 28.6%; Fig. 2*B*,*C*; synaptic density, 179 ± 3%; Fig. 2*D*). Similar to results obtained in Gα_{12}-knock-out neurons, specific knockdown of the endogenously expressed 5-HT$_7$ receptor with the siRNAs (Fig. 2*A*) significantly reduces the number of dendritic protrusions and synaptic density both under basal conditions as well as after 5-CT treatment (Fig. 2*B*–*D*). We also analyzed morphogenic and synaptogenic effects in hippocampal neurons isolated from Gα_{12}-deficient mice after their transfection with the 5-HT$_7$ receptor siRNA. Results of these experiments (Fig. 2*B*–*D*) demonstrate that the simultaneous switching off the 5-HT$_7$ receptor and G$_{12}$-protein does not result in any cumulative effects. Thus, both 5-HT$_7$ receptor and Gα_{12}-protein acting in the same signaling pathway are required for the induction of dendritic filopodia and synaptogenesis in hippocampal neurons. It is also notable that the 5-HT$_7$ receptor partly colocalized with the Gα_{12}-protein (Fig. 2*E*).

Effect of 5-HT$_7$R/G$_{12}$ signaling on neuronal functions

We next asked whether synaptic function of neurons is affected by the 5-HT$_7$ receptor agonist exposure. Spontaneous EPSPs and spontaneous firing activity were monitored using whole-cell recordings from hippocampal neurons cultured from P2 mice after 10 d in culture (Fig. 3*A*), close to the early developmental stage at which neurons form functional synaptic connections. Under control conditions, the EPSP frequency ranged from 0.03 to 2.4 Hz with a mean of 0.69 ± 0.11 Hz (Fig. 3*B*; $n = 29$). These values were similar in different preparations, indicating comparable developmental conditions. In neurons incubated with 5-CT (100 nM) during the last 4 d before recording, the EPSP frequency was significantly increased (Fig. 3*B*; 4.85 ± 0.53 Hz; $n = 33$; $p < 0.001$). Likewise, the spike frequency underwent a similar increase (0.06 ± 0.03 Hz in control vs 0.62 ± 0.15 Hz in 5-CT-treated neurons; $n = 19$; $p < 0.001$; Fig. 3*C*). We then analyzed synaptic functions in primary hippocampal neurons after knocking down endogenous 5-HT$_7$ receptor expression with siRNAs (Fig. 2*A*), as well as in neurons prepared from Gα_{12}-deficient mice. As shown in Figure 3, *B* and *C*, treatment of such neurons with 5-CT does not result in any significant changes of both EPSPs and spike frequency, further confirming the role of 5-HT$_7$R/G$_{12}$ signaling in obtained functional changes.

Because 5-CT is also a partial agonist for other serotonin receptors, including 5-HT$_{1A}$ and 5-HT$_5$ (Beer et al., 1992; Wood et al., 2000), it was important to assess the specific involvement of the 5-HT$_7$ receptor. Neurons were therefore treated with the selective 5-HT$_7$ receptor antagonist SB-269970 (1 μM), along with 5-CT. The treatment reduced both EPSP and the spike frequency to the control level (EPSP: 1.14 ± 0.17, $n = 16$; spike frequency, 0.02 ± 0.01 Hz; $n = 11$, Fig. 3*A*–*C*). These results suggest that activation of the 5-HT$_7$R/G$_{12}$ signaling pathway both enhances synaptogenesis and increases functional connectivity of hippocampal neurons.

In parallel, we analyzed the expression level of synaptic AMPARs, which provides an independent test of the electrophysiological data. Consistent with results of electrophysiological experiments, treatment of neurons with 5-CT increased both the total expression of AMPAR-positive puncta throughout cells and the numbers of synaptic AMPARs, as defined by the colocalization with synaptophysin (Fig. 3*D*,*E*; total AMPARs; 5-CT, 29.74 ± 4.74, $n = 40$, $p < 0.001$ compared with control, 9.36 ± 0.44, $n = 30$; Fig. 3*D*,*F*; synaptic AMPARs, 25.49 ± 3.69, $n = 40$, $p < 0.001$ compared with control, 8.25 ± 0.43). These effects were receptor specific, because they were abolished by treatment with an antagonist (Fig. 3*E*,*F*).

Effects of 5-HT$_7$R/G$_{12}$ signaling on neuronal morphology in organotypic hippocampal slices

The critical question for any results obtained in dissociated neuronal cultures is whether they can be reproduced in organized brain tissue. Therefore, we focused on organotypic slice cultures from the mouse hippocampus. In such preparations, the morphological organization of the hippocampus is mostly preserved, and the maturation of different cell types, synaptic contacts, and receptor expression are similar to those *in vivo* (Gähwiler et al., 1997; Gogolla et al., 2006). Organotypic slices were prepared from P5 mice and maintained for 5–6 d before analysis. During the last 4 d, the 5-HT$_7$ receptor agonist 5-CT (either alone or in combination with the antagonist SB-269970) was applied, and 1 d before analysis, slices were transfected with GFP to visualize and reconstruct 3D morphology of individual neurons (Herzog et al., 2006; Fig. 4*A*,*B*). We found that the 5-CT treatment resulted in a marked stimulation of spine formation, with no detectable changes to the typical morphology of individual dendritic spines. In 5-CT-treated neurons, the spine density was markedly increased compared with the control preparations

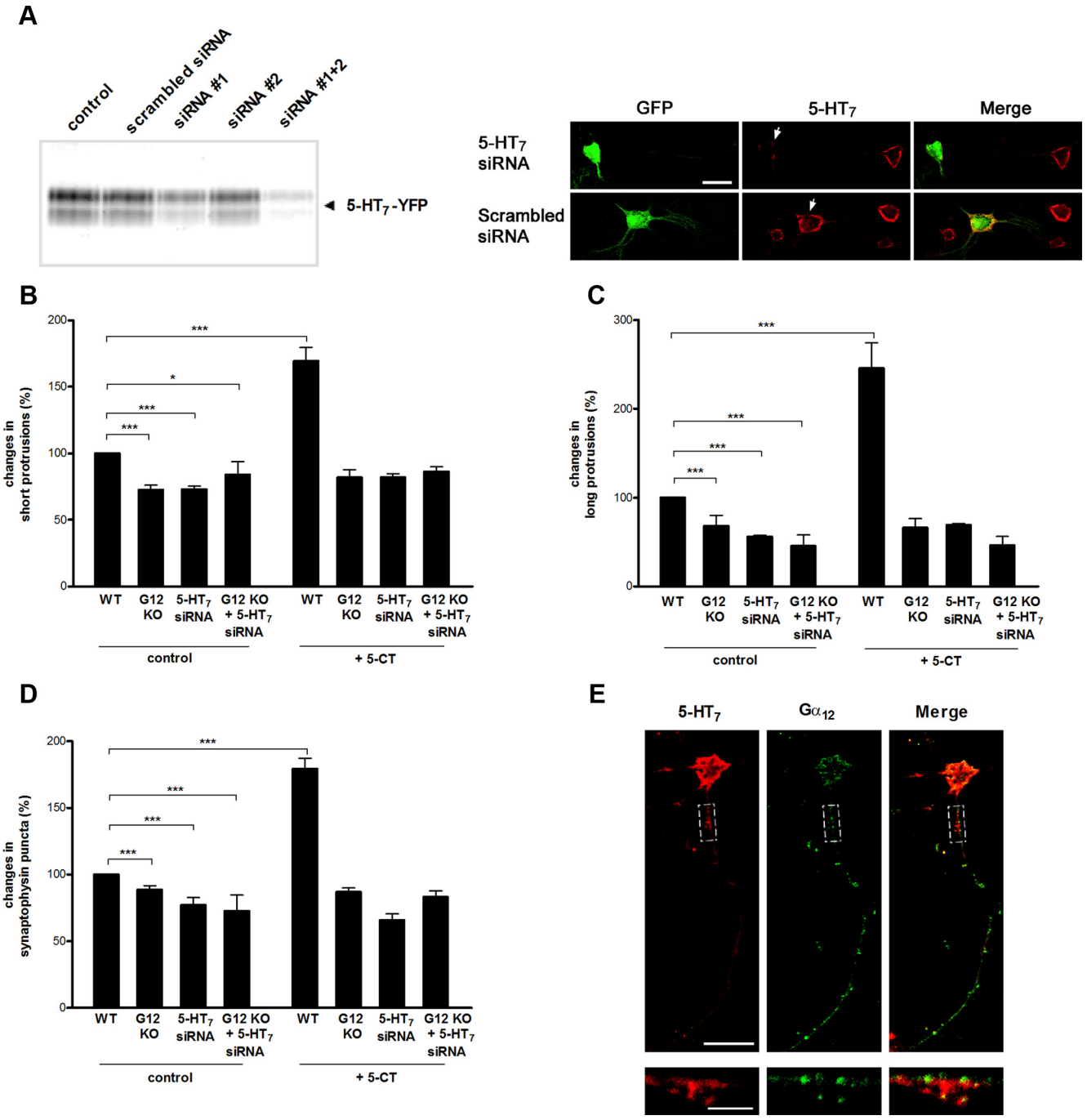

Figure 2. Morphogenic and synaptogenic effects of 5-CT are mediated by the 5-HT$_7$ receptor and Gα_{12}-protein. ***A***, Analysis of siRNA against the 5-HT$_7$ receptor. Left, The 5-HT$_7$-YFP receptor was expressed in neuroblastoma cells, which were cotransfected with scrambled or anti-5-HT$_7$ receptor siRNA constructs. A representative Western blot from three experiments is shown. Right, Expression of the 5-HT$_7$ receptor in hippocampal neurons after transfection with scramble and anti-5-HT$_7$ receptor siRNA is shown at DIV11. Expression vectors encoding for siRNA also contained GFP, allowing for simple identification of transfected neurons (arrows). Scale bar, 20 μm. ***B***, ***C***, The number of short (***B***) and long (***C***) dendritic protrusions is significantly decreased in untreated neurons isolated from the Gα_{12}-deficent mice, in wild-type neurons, where expression of endogenous 5-HT$_7$ receptor was knocked down by specific siRNA as well as in neurons from Gα_{12}-deficent mice after their transfection with 5-HT$_7$ receptor siRNA. After treatment with 5-CT, a significant increase in the number of both short and long protrusions is obtained only in neurons from the wild type, but neither in the Gα_{12}-deficient, in 5-HT$_7$ receptor siRNA-transfected neurons, nor in the Gα_{12}-deficient neurons after 5-HT$_7$ receptor siRNA transfection. Values represent mean ± SEM; *$p < 0.05$; ***$p < 0.001$. ***D***, The number of synapses is significantly decreased in untreated neurons isolated from Gα_{12}-deficient mice, in neurons transfected with 5-HT$_7$ receptor siRNA, and in Gα_{12}-deficient neurons after 5-HT$_7$ receptor siRNA transfection. Stimulation of the 5-HT$_7$ receptor with 5-CT does not result in any changes in the number of synapses in Gα_{12}-deficient neurons and in neurons without 5-HT$_7$ receptor. The number of dendritic protrusions and synaptophysin-positive puncta were calculated per 50 μm of dendrite. Values represent means ± SEM; ***$p < 0.001$ ($n = 30$). ***E***, Distribution of 5-HT$_7$ receptors and Gα_{12}-proteins in hippocampal neurons. Confocal images of hippocampal neurons at DIV11 are shown. The bottom high-magnification images represent a part of the dendrite shown by the dashed box. Scale bars: top, 20 μm; bottom, 5 μm. WT, Wild type; KO, knock-out.

(2.06 ± 0.11 vs 5.92 ± 0.09 spines per 50 μm of dendritic length; $p < 0.001$; Fig. 4*C*). The increase in the numbers of spines was 5-HT$_7$ receptor specific, because it was abolished by the selective receptor antagonist SB-269970 (3.45 ± 0.16 spines). In contrast, the surface area (0.67 ± 0.11 vs 0.83 ± 0.04 μm^2), length (2.85 ± 0.17 vs 2.75 ± 0.09 μm), diameter (0.20 ± 0.02 vs 0.20 ± 0.01 μm), and volume (0.039 ± 0.04 vs 0.042 ± 0.004 μm^3) of spines in neurons from 5-CT-treated preparations were similar to

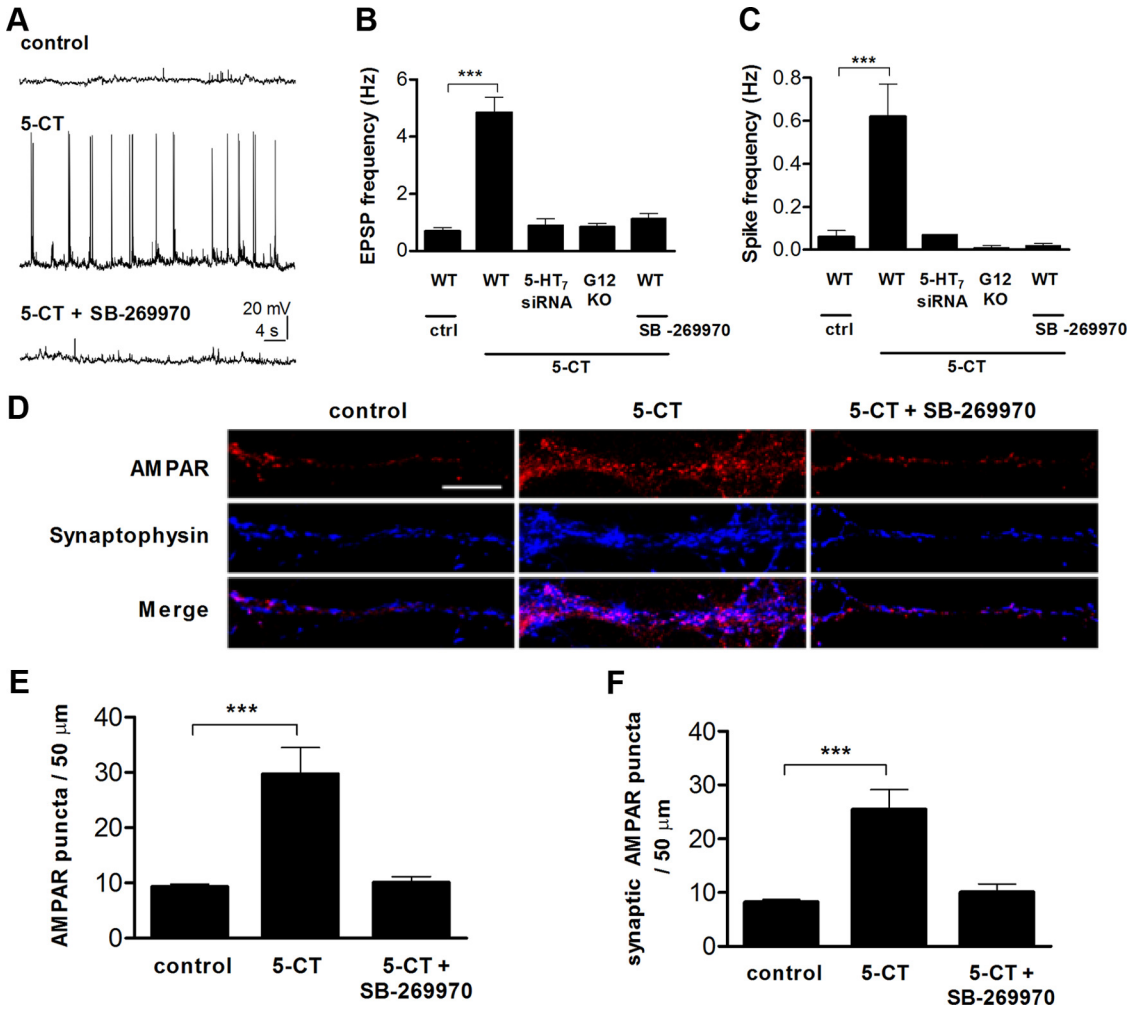

Figure 3. Stimulation of 5-HT$_7$R/G$_{12}$ signaling results in an increase of spontaneous neuronal activity. ***A***, Spontaneous neuronal activity was analyzed in primary cultures of hippocampal neurons by whole-cell patch-clamp recordings at DIV11. Representative recordings from control, 5-CT (100 nM), and 5-CT (100 nM) plus SB-269970 (1 μM) treated neurons are shown. In addition, effect of 5-CT treatment was analyzed in Gα_{12}-deficient neurons and in neurons transfected with 5-HT$_7$ receptor siRNA. The 5-CT and 5-CT plus SB-269970 treatment was performed during the last 4 d before recording. $V_{hold} = -65$ mV. ***B***, ***C***, Quantitative analysis of the frequency of EPSPs (***B***) and action potentials (***C***). Values represent means ± SEM; ***$p < 0.001$. ***D***, Representative images of neurons treated with 5-CT (100 nM) or 5-CT (100 nM) plus SB-269970 (1 μM). AMPARs and synaptophysin immunostaining is shown individually and as a merge. Scale bar, 10 μm. ***E***, ***F***, Average number of total surface (***E***) and synaptic AMPAR-positive (***F***) puncta per 50 μm of dendrite for control, 5-CT, and 5-CT plus SB-269970 treatments. Values represent means ± SEM; ***$p < 0.001$. WT, Wild type; KO, knock-out.

those of the control preparations, suggesting that the 5-HT$_7$R/G$_{12}$ signaling is critically involved in the formation of new spines rather than morphological transformation of existent spines.

To address whether similar changes in response to 5-CT might be occurring in intact tissue, we performed quantitative immunofluorescence studies by comparison of fluorescence intensity for synaptophysin, VGATs, and AMPARs in organotypic slices (Chao et al., 2007; Fig. 4*D*,*E*). Consistent with results obtained in dissociated neurons, intensity of synaptophysin immunostaining was significantly increased in hippocampal slices after prolonged stimulation of the 5-HT$_7$ receptor (Fig. 4*F*). Also, the total intensity of AMPARs was elevated after prolonged 5-CT treatment. In contrast, no changes were detected in the total intensity of VGAT, which is specific to the inhibitory GABAergic neurons (Fig. 4*F*). Changes in the amount and/or state of AMPA receptors at individual synapses have been suggested to correlate with the amplitude of miniature EPSCs (mEPSCs) (Lisman et al., 2007). Interestingly, the treatment with 5-CT (100 nM) for 4 d increased the average mEPSC amplitudes (43.37 ± 0.22 pA in control neurons, $n = 9$; 52.19 ± 0.3 pA in 5-CT-treated neurons, $n = 10$; $p < 0.01$), but we could not detect significant differences in the average mEPSC frequencies. Whereas the amplitude increase could indicate either an increased number of AMPARs available at individual synapses or an increased amount of glutamate released per discharge, the lack of statistically significant changes in the average mEPSC frequency is more difficult to interpret because it may simply reflect high variability of release probability among individual synapses across the preparations.

5-HT$_7$R/G$_{12}$ signaling modulates neuronal excitability and LTP

Our results demonstrate that stimulation of the 5-HT$_7$ receptor results in pronounced morphological and functional changes of individual hippocampal neurons. To determine whether these changes modulate functional plasticity of hippocampal networks, we performed additional electrophysiological recordings in organotypic slices prepared from P5 mice at DIV7. Four days before the analysis, slices were treated with a low concentration of 5-HT$_7$ receptor agonist 5-CT (100 nM). The effect of 5-HT$_7$

receptor-mediated signaling on synaptic transmission was analyzed using extracellular recordings of fEPSPs in the stratum radiatum of the CA1 region that were evoked by stimulation of Schaffer collaterals. First, IO curves were generated by plotting the amplitude of fEPSPs versus the stimulation intensity (Fig. 5*A*). Although the maximal responses obtained at higher stimulation intensity (100–150 μA) in the 5-CT-treated ($n = 12$) and in control ($n = 15$) slices were fairly similar, the average fEPSP amplitudes at low-stimulation strength (10–40 μA) were significantly increased in treated slices (Fig. 5*A*). There was a left shift of the IO curve, revealing that the same presynaptic stimulus elicited a larger postsynaptic response in the 5-CT-treated slices. When similar recordings were performed in organotypic preparations from Gα_{12}-deficient mice, the opposite effect was obtained (Fig. 5*A*). In this case, EPSP amplitudes at the low-stimulation intensity were decreased, resulting in a pronounced right shift of the IO curve compared with the control. To rule out changes in presynaptic fiber excitability as a possible reason for these effects, we compared presynaptic fiber volley amplitudes and did not observe any significant differences between control and 5-CT-treated slices. These combined data demonstrate the critical role of the G_{12}-protein as a downstream effector of 5-HT$_7$ receptor and also indicate that stimulation of 5-HT$_7$R/G_{12} signaling results in increased neuronal excitability (decreased threshold for the generation of evoked spikes).

To test whether the 5-CT-mediated enhancement of the fEPSP amplitudes occurs presynaptically or postsynaptically, we analyzed PPF, which is considered a presynaptic form of short-term plasticity. We found no difference in the PPF evoked using interstimulus intervals from 25 to 200 ms between control slices, 5-CT-treated slices, and slices from Gα_{12}-deficient mice (Fig. 5*B*). This result suggested a postsynaptic mechanism of the 5-HT$_7$ receptor-mediated enhancement of neuronal excitability.

The reduction in the population spike threshold in 5-CT-treated slices prompted us to investigate whether the induction of activity-dependent synaptic plasticity is also affected after stimulation of 5-HT$_7$R/G_{12} signaling. LTP was induced by high-frequency stimulation (100 Hz for 1 s) of Schaffer collaterals (Fig. 5*C*). In these experiments, 5-CT treatment markedly changed the induction of LTP (Fig. 5*C*). Already, the initial increase in the fEPSP slope (0–10 min) was significantly lower in 5-CT-treated than in control cultures. One hour after LTP induction, potentiation remained significantly decreased in 5-CT-treated cultures compared with controls (Fig. 5*C*). Together with the measurements of evoked fEPSPs (Fig. 5*A*), these data suggest that increased basal neuronal excitability mediated by the stimulation of the 5-HT$_7$R/G_{12} signaling pathway results in the preconditioning of synaptic transmission, leading to rapid LTP saturation and thus preventing further potentiation.

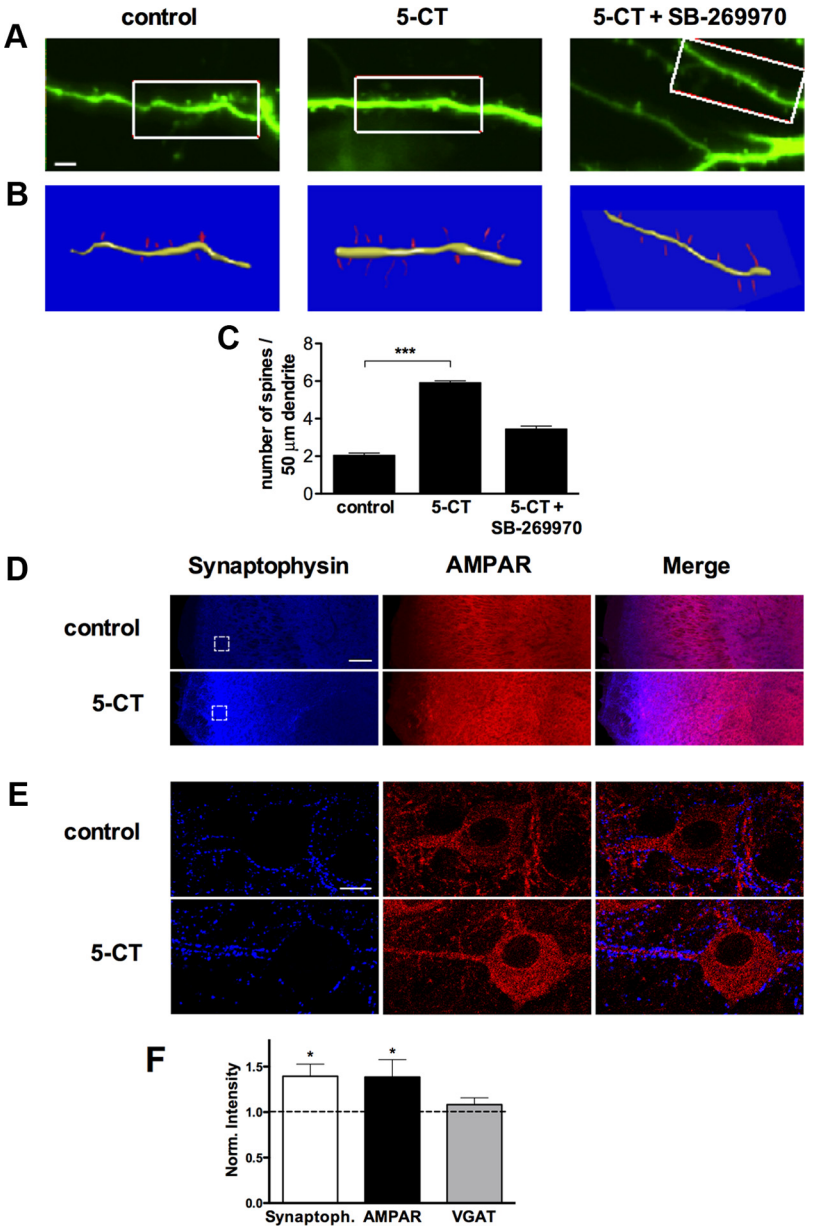

Figure 4. Stimulation of 5-HT$_7$R/G_{12} signaling promotes spinogenesis in organotypic hippocampal slices. ***A***, Organotypic slices from the hippocampus of a P5 mouse were treated with vehicle (H_2O, control), 5-CT (100 nM), or 5-CT plus SB-269970 (1 μM) at DIV2 for 4 d. The day before analysis, slices were transfected with GFP. A series of *z*-stacks were acquired for neurons expressing GFP. Scale bar, 5 μm. ***B***, Three-dimensional reconstructions were performed by using the method described by Herzog et al. (2006). ***C***, Bar graphs show the spine density calculated in control, 5-CT-treated, and 5-CT plus SB-269970-treated preparations. Data shown as mean ± SEM ($n = 30$). A statistically significant difference between values is indicated (***$p < 0.001$). ***D***, Representative images of the hippocampal CA1 region from control and 5-CT-treated organotypic preparations stained with anti-synaptophysin (blue) and anti-AMPAR (red) antibodies. Scale bar, 50 μm. ***E***, Larger magnifications of selected areas indicated in ***D***. Scale bar, 5 μm. ***F***, Bar graphs show synaptophysin, AMPAR, and VGAT intensity in 5-CT-treated hippocampal slides normalized to the control preparations (dashed line). Data shown as mean ± SEM. *$p < 0.05$.

Activation of 5-HT$_7$ receptors reduces postsynaptic Ca^{2+} entry evoked by either dendritic spikes or by synaptic activation

Whereas our data indicate profound consequences of 5-HT$_7$ receptor activation for sustained dendritic spine formation over days, it was important to understand the initial signaling cascade that trig-

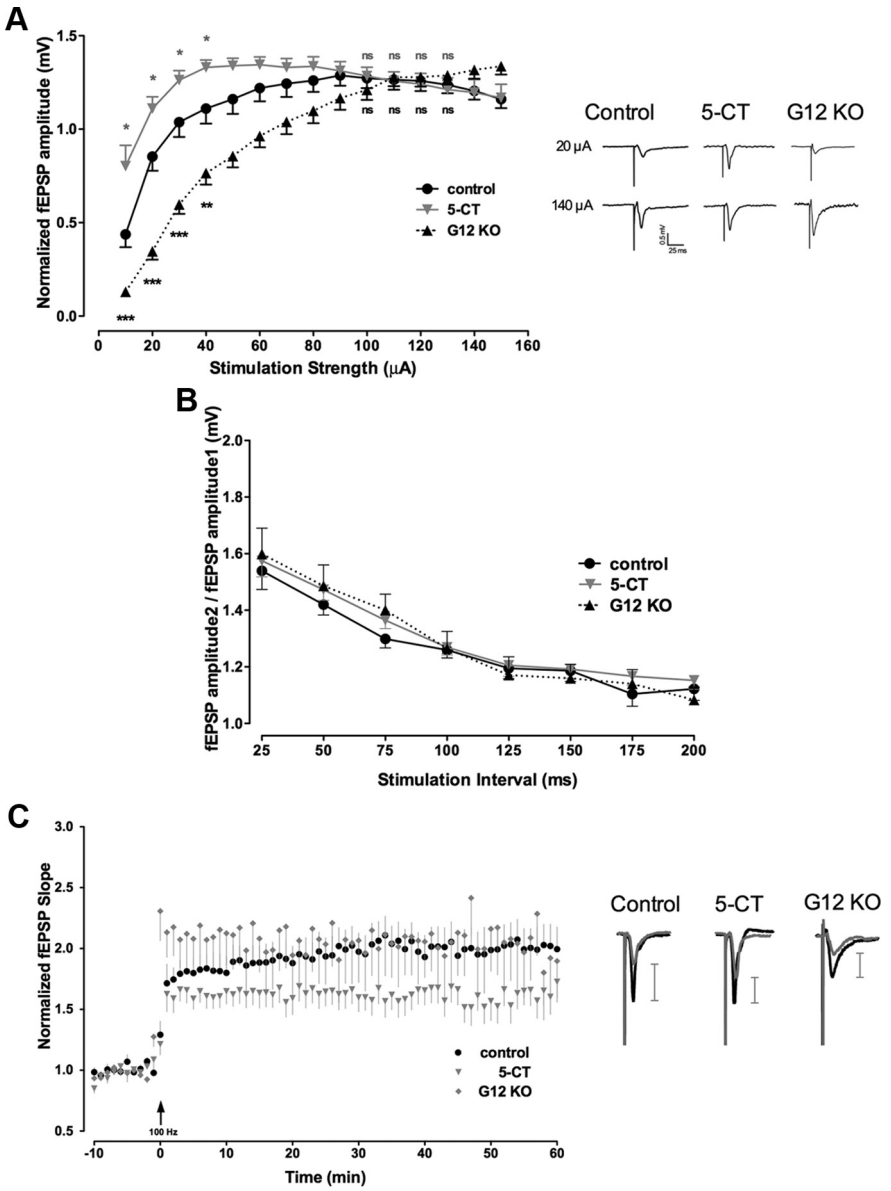

Figure 5. Stimulation of 5-HT$_7$R/G$_{12}$ signaling increases basal neuronal excitability and modulates synaptic plasticity. ***A***, Basal synaptic transmission in 5-CT-treated and control organotypic preparations, as well as from in cultures from Gα_{12}-deficient mice (G$_{12}$KO) measured as a relationship between the stimulus strength and amplitude of fEPSP from the Schaffer collateral–CA1 synapses. Although the maximal responses obtained at high-stimulation intensities (100–150 μA) in the 5-CT-treated ($n = 12$) and control ($n = 15$) slices are similar, the mean fEPSP amplitude at low-stimulation strengths (10–40 μA) is significantly increased in 5-CT-treated preparations and decreased in organotypic cultures from Gα_{12}-deficient mice ($n = 9$). Data are presented as mean ± SEM. A statistically significant difference between values is indicated (*$p < 0.05$; **$p < 0.01$; ***$p < 0.001$). Representative recordings of fEPSPs performed at 50% of maximal response (20 μA) and at maximal intensities (140 μA) are shown for control, 5-CT-treated, and Gα_{12} knock-out preparations on the right. ***B***, Analysis of PPF in CA1 synapses from the control, 5-CT-treated, and Gα_{12}-deficient mice preparations. ***C***, High-frequency stimulation (1 × 100 Hz for 1 s) of Schaffer collaterals in organotypic slices treated with 5-CT ($n = 12$) results in changed LTP of fEPSPs compared with control preparations ($n = 15$). Data shown are mean ± SEM of normalized fEPSPs. Representative recordings of fEPSPs performed at 50% of maximal response were evoked and recorded 5 min before (gray curves) and 50–60 min after (black curves) 1 × 100 Hz stimulation and are shown on the right for the control, 5-CT-treated, and Gα_{12} knock-out preparations. Scale bars on the right show the corresponding amplitude increment. LTP was determined as maximal responses between 50 and 60 min after the high-frequency stimulation ($n = 13$; $p < 0.01$). KO, Knock-out.

gers these changes after agonist application. Because postsynaptic Ca^{2+} entry is a major determinant of dendritic spine formation, motility, and stabilization (Lohmann and Wong, 2005; Oertner and Matus, 2005; Zheng and Poo, 2007), we asked whether activation of 5-HT$_7$ receptors exerts any direct effect on postsynaptic Ca^{2+} signaling. We therefore filled CA1 pyramidal cells in whole-cell mode with the morphological tracer Alexa Fluor 594 and the Ca^{2+} indicator Fluo-4 (Fig. 6*A*) and used two-photon excitation microscopy routines, as detailed previously (Scott et al., 2008), to monitor postsynaptic Ca^{2+} in acute hippocampal slices. First, we examined Ca^{2+} transients evoked by the back-propagating action potentials in individual dendritic spines and shafts (Fig. 6*B*). Second, we focused on individual dendritic spines of CA1 pyramidal cells and documented (NMDA receptor-dependent) intraspine Ca^{2+} transients evoked, in a probabilistic manner, by electrical stimuli applied to presynaptic Schaffer collaterals (Fig. 6*C*). This mode of observation, termed "optical quantal analysis," enables direct readout of both release probability P_r and glutamate release-induced postsynaptic Ca^{2+} entry at individual identified connections (Oertner et al., 2002; Emptage et al., 2003; Fig. 6*C*,*D*).

First, we found that within a few minutes of application, 5-CT reduced the spike-evoked transient Ca^{2+} responses by 48 ± 8% in dendritic spines ($n = 9$; $p < 0.005$) and by 25 ± 4% in dendritic shafts ($n = 5$; $p < 0.05$; Fig. 6*E*). In parallel, 5-CT induced an outward current (33 ± 6 pA; $n = 6$), indicating significant membrane hyperpolarization, which was consistent with the effects of 5-CT in these cells reported previously (Pugliese et al., 1998). This result suggests that the signaling mechanism of 5-HT$_7$ receptor action involves a reduction in spike-evoked postsynaptic Ca^{2+} entry and that the concurrent changes in membrane excitability (and therefore spike propagation mechanisms) contribute to these effects. Second, activation of 5-HT$_7$ receptors had no effect on P_r at individual synapses (0.45 ± 0.06 and 0.42 ± 0.05 in baseline conditions and in 5-CT, respectively; $n = 6$; $p > 0.2$; Fig. 6*F*, left), thus pointing to the postsynaptic origin of the mechanisms involved. At the same time, however, the average postsynaptic Ca^{2+} entry was significantly reduced by the 5-HT$_7$ agonist 5-CT (by 17 ± 4%; $n = 6$; $p < 0.011$; Fig. 6*F*, right). Although the precise dissection of the underlying receptor–channel mechanism requires a separate study, this result provides important evidence that activation of 5-HT$_7$ receptors reduces the postsynaptic Ca^{2+} signal triggered by neurotransmitter release at individual excitatory synapses (see Discussion).

Expression of 5-HT$_7$ receptor and Gα_{12}-protein decreases dramatically during postnatal development

It has been suggested that different effects of serotonin during development may be mediated by the variable expression of the

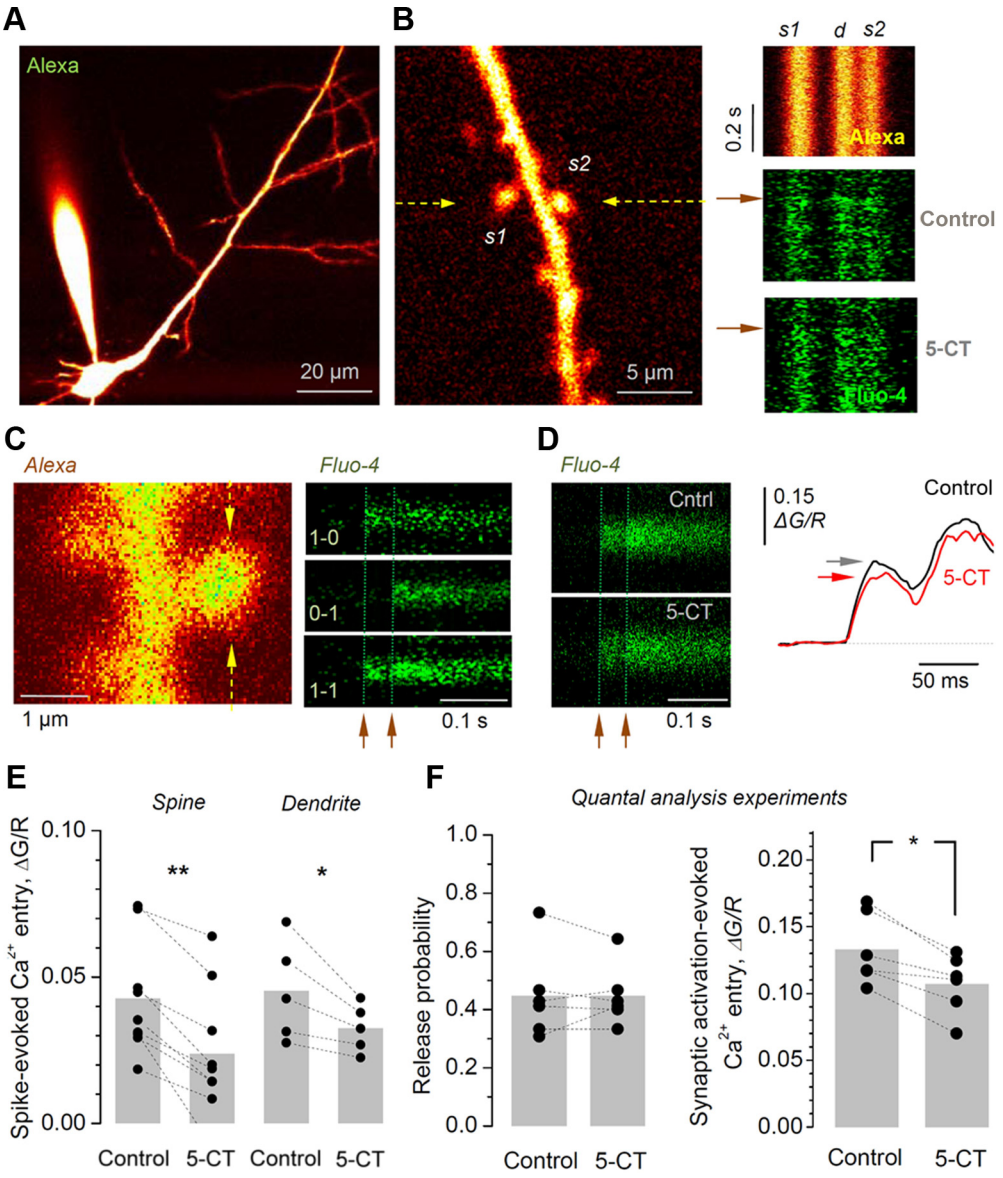

Figure 6. In acute hippocampal slices, activation of 5-HT$_7$ receptors reduces postsynaptic Ca^{2+} entry evoked by either backpropagating action potentials or by synaptic activation, while having no effect on evoked release probability. ***A***, CA1 pyramidal cells are loaded with the tracer Alexa 594 (50 μM) and the Ca^{2+} indicator Fluo-4 (400 μM). ***B***, Left, An example of a spiny dendritic fragment of interest is selected for imaging, with two spines (s1 and s2) recorded using line scan recording (arrows indicate position); Alexa channel, $\lambda_x^{2p} = 800$ nm. Right, Examples of line scans (500 Hz) from the dendritic fragment depicted in on the left during generation of a backpropagating action potential (onset is shown by the arrows; two spines and dendritic stem traces are marked as s1, s2, and d, respectively) recorded in "red" Alexa channel (top), and in "green" Fluo-4 channel (middle) in control conditions and 5 min after application of 100 nM 5-CT (bottom), as indicated. ***C***, Optical quantal analysis at CA1–CA3 synapses. Left, Characteristic image of a dendritic fragment with prominent spines (Alexa channel; arrows, line scan position). Right, Examples of Ca^{2+}-sensitive responses recorded (500 Hz line scan) from the spine head shown on the left after two stimuli (arrowheads, 50 ms apart) applied to Schaffer collaterals; three typical cases of stochastic responses are shown, with 0 and 1 indicating, respectively, signal failures and successes after each stimulus. ***D***, Left, Average postsynaptic Ca^{2+} entry evoked in the dendritic spine shown in ***C*** by successful synaptic activation (failures excluded; arrowheads show stimulus onset) in control conditions (top) and 15 min after 5-CT application (bottom). Right, The two corresponding profiles, as indicated, expressed as Ca^{2+} (green) channel values related to the Alexa (red) values ($\Delta G/R$), to cancel out artifact fluorescence fluctuations caused by focus drift; horizontal arrows indicate the first response amplitude. ***E***, Statistical summary of experiments shown in ***B***: average $\Delta G/R$ responses (Fluo-4/Alexa channel ratio integrated over 6–26 ms after spike in individual sweeps, subsequently averaged over 10–15 trials) recorded in individual dendritic spines ($n = 9$) and adjacent dendritic stems ($n = 5$), before and after 5-CT application, as indicated. Individual experiments are shown by dots connected by a dotted line. Gray bars indicate a sample average. $^{**}p < 0.01$; $^{*}p < 0.05$. ***F***, Summary of experiments shown in ***C*** and ***D***. Activation of 5-HT$_7$ receptors has no effect on release probability (0.45 ± 0.06 and 0.42 ± 0.05 in baseline conditions and in 5-CT, respectively; $n = 6$; $p > 0.2$; left) while decreasing the average Ca^{2+} entry evoked by activation of individual synapses (by $17 \pm 4\%$; $n = 6$; $p < 0.011$; right).

corresponding receptors and/or their downstream effectors (Bonnin et al., 2006, 2007). Therefore, we next determined the expression profile for both 5-HT$_7$ receptor and Gα_{12}-protein in the mouse hippocampus at different stages of postnatal development using real-time quantitative RT-PCR. This approach demonstrated that 5-HT$_7$ receptor transcripts were strongly expressed during early postnatal stages (P2 and P6) and dramatically downregulated (up to ninefold) during later development. A similar expression profile was obtained for the Gα_{12}-protein (Fig. 7*A*). In contrast, the expression level of the Gα_s-protein, which can also be activated by 5-HT$_7$ receptor, was not significantly modulated during development (Fig. 7*A*). Furthermore, expression analysis of another G_S- and $G_{12/13}$-coupled serotonin receptor, 5-HT$_4$ (Ponimaskin et al.,

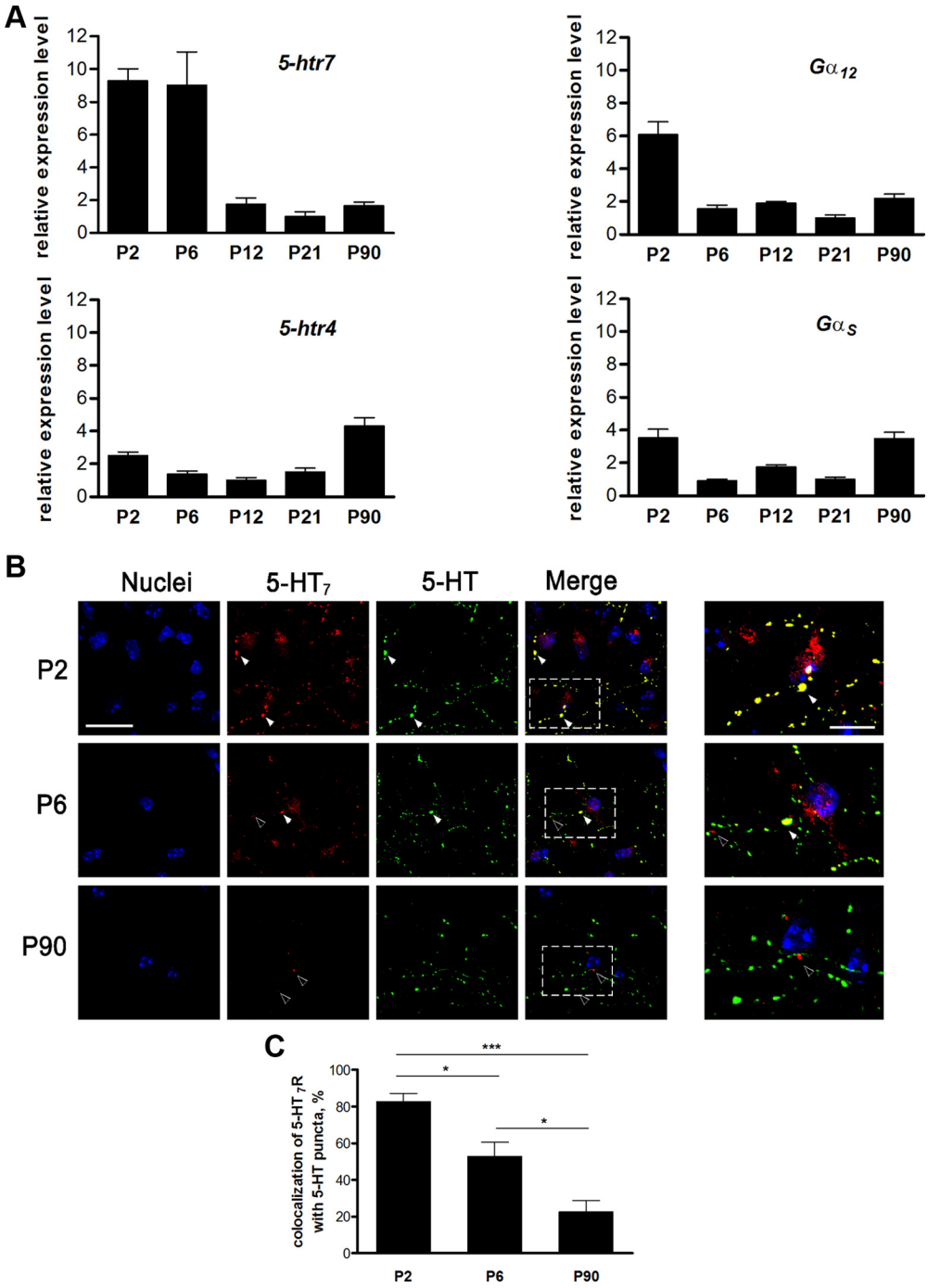

Figure 7. Expression of the 5-HT$_7$ receptor and the Gα_{12}-protein decreases during postnatal development. ***A***, Relative changes in the amount of mRNA encoding for the 5-HT$_7$ receptor and the Gα_{12}-protein, as well as the 5-HT$_4$ receptor and the Gα_s-protein, in the mouse hippocampus were determined at different stages of the postnatal development using real-time quantitative RT-PCR and $\Delta\Delta C_t$ method. The 5-HT$_7$ receptor and Gα_{12}-protein are strongly expressed at early postnatal stages and are downregulated during later stages of development. ***B***, Distribution of 5-HT$_7$ receptor and 5-HT in hippocampus during development. Representative images of hippocampal cryosections obtained from P2, P6, and P90 mice are shown. Colocalization of 5-HT$_7$ receptor and 5-HT is shown by white arrows. During later stages of development, the amount of the 5-HT$_7$ receptor is decreased, and receptor colocalization with 5-HT-positive varicosities is reduced (black arrows). Scale bar, 20 μm. Right images show the high magnification of the regions of interest shown in merged images. Scale bar, 5 μm. ***C***, colocalization of dendritic 5-HT$_7$ receptor-positive clusters with 5-HT-positive puncta at different developmental stages. Values represent means $\pm$ SEM; $^*p < 0.05$; $^{***}p < 0.001$ ($n = 30$).

2002), revealed that the amount of receptor mRNA does not undergo strong variation during development (Fig. 7*A*). Immunohistochemical analysis confirmed a higher expression of 5-HT$_7$ receptor in the CA1 region during early postnatal stages (P2 and P6) compared with P90 (Fig. 7*B*). Moreover, we observed a high degree of colocalization between the 5-HT$_7$ receptor and 5-HT-containing varicosities at P2 stages, whereas both expression and colocalization of the 5-HT$_7$ receptor with serotonergic fibers was continuously decreased during later developmental stages (Fig. 7*B*,*C*). These data demonstrate that 5-HT$_7$ receptor and Gα_{12}-protein display dynamic expression patterns characterized by a strong, but transient, expression during early postnatal stages of hippocampal development.

The effects of 5-HT$_7$R/G$_{12}$ signaling are restricted to the early developmental stages

Decreased expressions of 5-HT$_7$ receptor and Gα_{12}-protein during the later postnatal stages suggest that the morphological and functional effects observed in juvenile hippocampal neurons after stimulation of 5-HT$_7$ receptor may be diminished in adult mice. Therefore, we next investigated the role of 5-HT$_7$R/G$_{12}$ signaling in dendritic morphogenesis and synaptogenesis in cultures of dissociated hippocampal neurons at DIV21. Similarly to analysis presented in Figure 1, these neurons were incubated with 5-CT (100 nM) during the last 4 d before analysis. In contrast to results obtained after treatment of younger cultures (DIV5; Fig. 1*C–E*), agonist treatment started at DIV21 does not result in any significant changes in the number of dendritic protrusions compared with the nontreated controls (Fig. 8*A*,*B*). The number of SPs per 50 μm of dendritic length was 14.75 $\pm$ 3.51 in control versus 14.06 $\pm$ 2.71 after 5-CT treatment ($n = 30$), and the number of LPs (over 10 μm) was 0.49 $\pm$ 0.17 in control versus 0.5 $\pm$ 0.13 after 5-CT treatment ($n = 30$). Also, the number of synaptophysin-positive puncta per 50 μm of dendrite was not affected after treatment of neurons with 5-CT (17.29 $\pm$ 2.32 vs 17.18 $\pm$ 2.24 in control; $n = 30$; Fig. 8*C*).

To determine whether 5-HT$_7$R/G$_{12}$ signaling can modulate functional plasticity of hippocampal networks in adult animals, we performed electrophysiological experiments using 10-week-old male mice that have been chronically treated with the highly selective 5-HT$_7$ receptor antagonist SB656104-A. SB656104-A penetrates the blood–brain barrier, and its pharmacokinetic properties are well characterized (Thomas et al., 2003). Animals were treated for 3 weeks twice daily by intraperitoneal injection of 20 mg kg^{-1}. An analysis of neuronal excitability and synaptic plasticity (LTP) in acute slices obtained from the antagonist-treated mice did not reveal significant changes of basal excitability and the average magnitude of LTP compared with untreated controls (Fig. 8*D*,*E*). These combined results demonstrate that stimulatory effects of 5-HT$_7$R/G$_{12}$ signaling on spinogenesis and synaptogenesis, as well as on synaptic plasticity, are restricted to early postnatal development stages.

Experiments in Gα_{12}-deficient mice demonstrated that G$_{12}$-protein is required for the obtained morphological and functional effects (Figs. 2, 5). On the other hand, a decrease in the Gα_{12} expression during development suggests that the time window for G$_{12}$ action is restricted to early postnatal stages. To verify this suggestion, we compared the morphology of hippocampal neurons in wild-type and Gα_{12}-deficient mice at different developmental stages by visualizing CA1 pyramidal neurons after retrograde DiI labeling (Morita et al., 2009; Fig. 8*F*,*G*). At P6, the number of short dendritic protrusions measured per 50 μm of dendrite in neurons of Gα_{12}-deficient mice was reduced to 14.60 $\pm$ 0.60 compared with 26.98 $\pm$ 2.32 in wild-type animals ($p < 0.001$; Fig. 8*F*). In contrast, the spine density was not significantly different in hippocampal neurons of 10-month-old mice (64.79 $\pm$ 1.93 in wild type, 62.59 $\pm$ 3.64 in Gα_{12}-deficient mice; Fig. 8*G*). Thus, loss of Gα_{12} results in a drastic reduction of spine density at the early postnatal stages, whereas this effect becomes completely compensated by G$_{12}$-independent mechanisms at adulthood.

Discussion

5-HT$_7$R/G$_{12}$ signaling modulates formation and functioning of synapses

It is widely accepted that patterns of neuronal activity play a major role in reorganization of neuronal connection and circuits (Katz and Shatz, 1996; Maletic-Savatic et al., 1999; Jontes and Smith, 2000). However, mechanisms underlying formation of the initial population of synaptic connections, i.e., before any network activity could be established, are far from being completely understood. Over the past several years, it has become evident that serotonin may modulate different aspects of early neuronal differentiation, including neurite outgrowth and synaptogenesis, before it acts as a neurotransmitter (Mazer et al., 1997; Udo et al., 2005). The morphogenic functions of serotonin may be mediated by a variety of 5-HT receptor subtypes (Barnes and Sharp, 1999; Hoyer et al., 2002), and we have previously showed that activation of the 5-HT$_7$ receptor promoted neurite outgrowth in hippocampal neurons (Kvachnina et al., 2005).

In the present study, we demonstrated that prolonged stimulation of the 5-HT$_7$ receptor leads to a pronounced increase in the number of dendritic protrusions. It has been proposed that dendritic protrusions actively participate in the formation of synapses and that initial synaptogenesis may be the result of contacts between dendritic protrusions and axons (Mattila and Lappalainen, 2008). Supporting this view, we found that the number of identified excitatory synapses was also increased after stimulation of the 5-HT$_7$ receptor. We found a similar morphogenic function of the 5-HT$_7$ receptor in organized brain circuitries (organotypic slice preparation), where stimulation of 5-HT$_7$ receptor caused a pronounced elevation of spinogenesis without affecting spine shape and size.

The 5-HT$_7$ receptor-mediated boost in synaptogenesis results in marked enhancement of spontaneous neuronal activity (e.g., EPSP and spike frequency) generated in networks formed by the cultured hippocampal neurons. In slices, the receptor-mediated facilitation of spinogenesis was accompanied by an increase in basal neuronal excitability as assessed by the analysis of fEPSPs. The coordinated changes in synaptogenesis and synaptic excitability obtained here can represent a mechanism responsible for the generation of initial synaptic connections and maturation of basal synaptic circuits during early neuronal development. It is noteworthy that synaptic plasticity was also modulated in a way that the 5-HT$_7$ receptor-mediated increase in basal excitability resulted in quick saturation of LTP, therefore preventing further potentiation (Saghatelyan et al., 2001; Jedlicka et al., 2009).

Underlying mechanisms of 5-HT$_7$R/G$_{12}$ signaling are Ca^{2+} dependent

The 5-HT$_7$ receptor is coupled to two different heterotrimeric G-proteins, G$_s$ and G$_{12}$ (Vanhoenacker et al., 2000). Both the G$_s$ and G$_{12}$ proteins can then regulate the cellular morphology by activating different signaling cascades. In the case of G$_s$, morphogenic effects are mediated either by the modulation of the cAMP level (Iyengar, 1996; Corset et al., 2000) or by the direct binding of Gα_s subunits to the cytoskeleton (Yu et al., 2009). Downstream effectors of the G$_{12}$-protein-mediated changes in the actin cytoskeleton are members of the Rho family of small GTPases, including RhoA, Rac1, and Cdc42 (Jaffe and Hall, 2005). Experiments with 5-HT$_7$ receptor siRNA, together with data from Gα_{12}-deficient mice, revealed that the coupling of 5-HT$_7$ receptor to G$_{12}$-protein is essential for morphological and functional effects obtained in the present study. We have recently demonstrated that small GTPases RhoA and Cdc42 represent the main downstream effectors of the 5-HT$_7$R/G$_{12}$ signaling and also found that the major functional effects of this pathway are mediated by the activation of the Cdc42 (Kvachnina et al., 2005).

In the present study, we found that activation of 5-HT$_7$ receptors has no effect on evoked release probability while decreasing

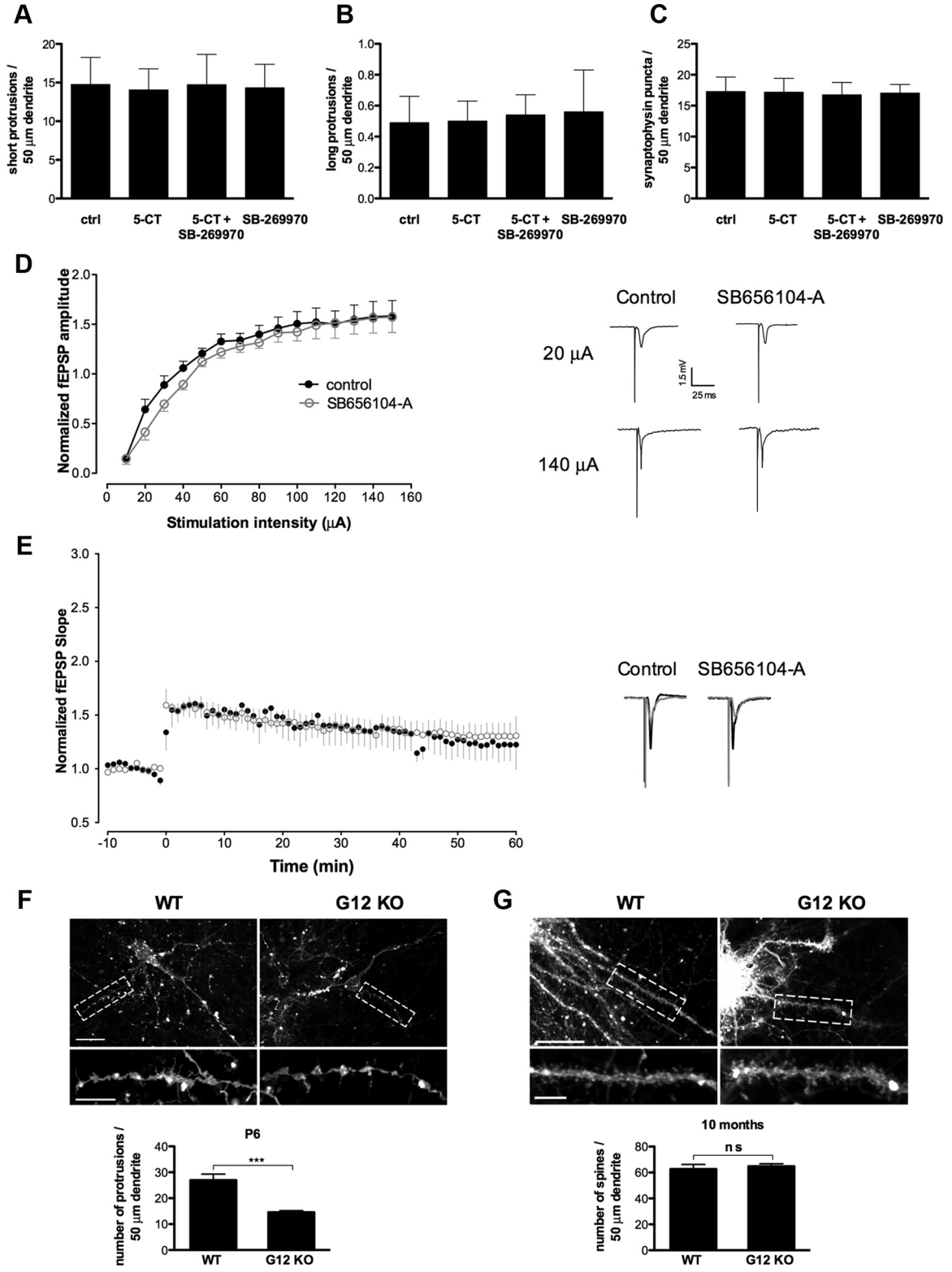

Figure 8. Effects of 5-HT$_7$R/G$_{12}$ signaling are restricted to the early developmental stages. ***A–C***, Stimulation of the 5-HT$_7$ receptor in culture of dissociated hippocampal neurons at DIV21 has no effect on formation of short (<10 μm; ***A***) and long (>10 μm; ***B***) dendritic protrusions and on the number of synaptophysin-positive puncta (***C***). The number of dendritic protrusions and synaptophysin-positive puncta are calculated per 50 μm of dendrite. Values represent means ± SEM; $n = 30$. ctrl, Control. ***D***, Basal synaptic transmission in acute hippocampal slices prepared from the control mice and mice treated with the 5-HT$_7$ receptor antagonist SB656104-A is shown as a relationship between the stimulus intensity and fEPSP amplitude. The maximal responses obtained at low and high stimulation intensities in slices from the SB656104-A-treated ($n = 7$) and control ($n = 8$) animals are similar. Recordings of fEPSPs performed at 20 and 140 μA are shown on the right. ***E***, High-frequency stimulation of Schaffer collaterals in hippocampal slices from SB656104-A ($n = 7$) and control ($n = 8$) animals results in LTP of fEPSPs. Representative recordings of fEPSPs performed at 50% of maximal response were evoked and recorded 5 min before (gray curves) and 50–60 min after (black curves) high-frequency stimulation and are shown for control and antagonist-treated mice on the right. ***F***, ***G***, Representative images of DiI-labeled apical dendrites of CA1 pyramidal neurons in hippocampal slices (top) are shown together with the quantification of the density of dendritic protrusions (bottom) from P6 (***F***) and 10-month-old (***G***) wild-type and Gα_{12}-deficient mice. ***$p < 0.001$. WT, Wild type; KO, knock-out.

synaptically evoked Ca^{2+} entry in postsynaptic dendritic spines, which can be mediated either by inhibition of voltage-dependent Ca^{2+} channels via G$\beta\gamma$ subunits (Jeong and Ikeda, 1999) or by modulation of T-type Ca^{2+} channels via the activated Rho-associated kinase ROCK (Iftinca et al., 2007). It has been shown that a reduction in postsynaptic calcium entry induces growth of dendritic filopodia (precursors of dendritic spines) (Lohmann and Wong, 2005) and increases motility of fully formed spines, possibly by modulating intraspine assembly of the filamentous actin (Oertner and Matus, 2005; Zheng and Poo, 2007). Conversely, local calcium uncaging (Lohmann and Wong, 2005) or increased postsynaptic Ca^{2+} entry has been associated with reduced filopodial motility and with stabilization of spine morphology (Oertner and Matus, 2005; Zheng and Poo, 2007), and even with rapid contraction of spines during postsynaptic spike bursts (Korkotian and Segal, 2001). Furthermore, it has been demonstrated that Ca^{2+} influx in dendrites leads to strong activation of RhoA, which results in the arrest of neurite regeneration, neurite retraction, and induction of the excitotoxic pathway (Semenova et al., 2007). Therefore, the 5-HT$_7$ receptor-mediated reduction of [Ca^{2+}] may result in profound local inhibition of RhoA, whereas the receptor-mediated Cdc42 activation will not be affected. These combined data suggest that 5-HT$_7$ receptor-mediated activation of Cdc42 paralleled by RhoA inhibition represents a mechanism responsible for the formation of dendritic protrusions and spines in hippocampal neurons. Future studies involving experiments with 5-HT$_7$ receptor-deficient mice will be needed to more precisely evaluate the contribution of small GTPases and receptor-regulated [Ca^{2+}] as down-stream effectors in 5-HT$_7$R/G$_{12}$-mediated signaling.

Physiological importance of 5-HT$_7$R/G$_{12}$ signaling

There is a growing evidence that 5-HT can act not only as a neurotransmitter but is also involved in the regulation of different aspects of early neuronal development. The early actions of 5-HT include modulation of neuronal differentiation, synaptogenesis, axonal pathfinding, as well as effects on cell migration and morphogenesis of the cortex (Okado et al., 1993; Bennett-Clarke et al., 1994; Mazer et al., 1997; Gould, 1999; Bonnin et al., 2007). Moreover, transient modifications of the serotonergic system (e.g., by stress), especially during early postnatal development, seems to influence brain morphology as well as cognitive and emotional behaviors in adulthood (Mazer et al., 1997; Gross et al., 2002; Ansorge et al., 2004). Molecular mechanisms underlying such developmental effects of 5-HT are poorly understood. The high variability of reported effects suggests, however, that different 5-HT actions during development may be defined by the variable expression of the corresponding receptor subtypes and/or their downstream effectors. First experimental evidence for such effects has recently been reported (Bonnin et al., 2006, 2007), demonstrating that dynamic expression of 5-HT$_1$ receptor subfamily members in the telencephalon of the prenatal mouse may be responsible for the serotonin-mediated modulation of responsiveness of embryonic thalamocortical axons to netrin-1. It has been also shown that coordinated changes in expression of 5-HT$_7$ and 5-HT$_{1A}$ receptors during early postnatal development are critically involved in regulation of receptor functions in developing prefrontal cortex (Béïque at al., 2004). Moreover, transient depletion of the 5-HT$_{1A}$ receptor during early development has been shown to be responsible for altered behavior in the adult (Gross et al., 2002). Similarly, transient inactivation of 5-HT transporter during early developmental stages resulted in abnormal behavior in adult mice (Ansorge et al., 2004).

In the present study, we found that the expression levels of both 5-HT$_7$ receptor and Gα_{12}-protein in the hippocampus was progressively decreased during the postnatal development. Consistent with this observation, stimulatory effects of 5-HT$_7$R/G$_{12}$ signaling on spinogenesis and synaptogenesis, as well as on synaptic plasticity, were restricted to early postnatal development stages and abolished in adult mice. Therefore, regulated expression of the 5-HT$_7$R/G$_{12}$ signaling pathway players may represent a mechanism by which serotonin specifically modulates formation of basal neuronal connections during the early postnatal development. This is supported by several observations. First, analysis of Gα_{12}-deficient mice revealed that G$_{12}$-protein is required for spinogenesis only at early postnatal stages. Second, the serotonergic system is one of the earliest neurotransmitter systems in the mammalian brain, with the final arborization of serotonergic innervation occurring up to postnatal day 21 (Lidov and Molliver, 1982; Lauder, 1990). During the terminal serotonergic field development (embryonic day 19 to P21), 5-HT reaches the highest concentration in the brain (Whitaker-Azmitia, 2005). Moreover, in the mouse hippocampus, we observed a high degree of colocalization between serotonin-containing varicosities and the 5-HT$_7$ receptor during early postnatal stages, which provide a morphological basis for the selective activation of the 5-HT$_7$R/G$_{12}$ signaling pathway.

In addition to the role of 5-HT$_7$R/G$_{12}$ signaling in formation of basal neuronal networks during early development, this pathway may also be implicated in physiological response to external stimuli, in particular to prenatal stress. It is well known that early stress can cause hippocampal damages characterized by synaptic loss and atrophy (McEwen, 1999; Tata and Anderson, 2010), and these changes are accompanied by reduced hippocampal 5-HT concentration (Hayashi et al., 1998). It has also been shown that treatment of prenatally stressed mice with selective serotonin reuptake inhibitor (SSRI) reversed stress-mediated dysfunctions, leading to normal response to stress and to increased synaptic density in the hippocampus (Ishiwata et al., 2005). Interestingly, the restorative SSRI effect was only apparent at the early postnatal stages (weeks 1–3), whereas treatment of adult animals did not produce any effect. This correlates well with our data on regulated expression of 5-HT$_7$ receptor and G$_{12}$-protein, suggesting that the 5-HT$_7$R/G$_{12}$ signaling pathway may represent a potential target for treatment of stress-evoked dysfunctions.

Thus, 5-HT-induced activation of the 5-HT$_7$R/G$_{12}$ signaling pathways and the consequent reorganization of the dendritic morphology seem to be a part of the molecular cascade required for the growth of new synapses and the formation of initial neuronal networks, which then become the subject of activity-dependent structural and functional plasticity (Citri and Malenka, 2008; Turrigiano, 2008).

References

Ansorge MS, Zhou M, Lira A, Hen R, Gingrich JA (2004) Early-life blockade of the 5-HT transporter alters emotional behavior in adult mice. Science 306:879–881.

Azmitia EC (2001) Modern views on an ancient chemical: serotonin effects on cell proliferation, maturation, and apoptosis. Brain Res Bull 56:413–424.

Barnes NM, Sharp T (1999) A review of central 5-HT receptors and their function. Neuropharmacology 38:1083–1152.

Bartrup JT, Moorman JM, Newberry NR (1997) BDNF enhances neuronal growth and synaptic activity in hippocampal cell cultures. Neuroreport 8:3791–3794.

Beer MS, Stanton JA, Bevan Y, Chauhan NS, Middlemiss DN (1992) An investigation of the 5-HT1D receptor binding affinity of 5-hydroxytryptamine,

5-carboxyamidotryptamine and sumatriptan in the central nervous system of seven species. Eur J Pharmacol 213:193–197.

Béïque JC, Campbell B, Perring P, Hamblin MW, Walker P, Mladenovic L, Andrade R (2004) Serotonergic regulation of membrane potential in developing rat prefrontal cortex: coordinated expression of 5-hydroxytryptamine (5-HT)1A, 5-HT2A, and 5-HT7 receptors. J Neurosci 24:4807–4817.

Bennett-Clarke CA, Leslie MJ, Lane RD, Rhoades RW (1994) Effect of serotonin depletion on vibrissa-related patterns of thalamic afferents in the rat's somatosensory cortex. J Neurosci 14:7594–7607.

Bonnin A, Peng W, Hewlett W, Levitt P (2006) Expression mapping of 5-HT1 serotonin receptor subtypes during fetal and early postnatal mouse forebrain development. Neuroscience 141:781–794.

Bonnin A, Torii M, Wang L, Rakic P, Levitt P (2007) Serotonin modulates the response of embryonic thalamocortical axons to netrin-1. Nat Neurosci 10:588–597.

Chao HT, Zoghbi HY, Rosenmund C (2007) MeCP2 controls excitatory synaptic strength by regulating glutamatergic synapse number. Neuron 56:58–65.

Citri A, Malenka RC (2008) Synaptic plasticity: multiple forms, functions, and mechanisms. Neuropsychopharmacology 33:18–41.

Corset V, Nguyen-Ba-Charvet KT, Forcet C, Moyse E, Chédotal A, Mehlen P (2000) Netrin-1-mediated axon outgrowth and cAMP production requires interaction with adenosine A2b receptor. Nature 407:747–750.

De Paola V, Arber S, Caroni P (2003) AMPA receptors regulate dynamic equilibrium of presynaptic terminals in mature hippocampal networks. Nat Neurosci 6:491–500.

Dityatev A, Dityateva G, Schachner M (2000) Synaptic strength as a function of post- versus presynaptic expression of the neural cell adhesion molecule NCAM. Neuron 26:207–217.

Emptage NJ, Reid CA, Fine A, Bliss TV (2003) Optical quantal analysis reveals a presynaptic component of LTP at hippocampal Schaffer-associational synapses. Neuron 38:797–804.

Fiorica-Howells E, Maroteaux L, Gershon MD (2000) Serotonin and the 5-HT(2B) receptor in the development of enteric neurons. J Neurosci 20:294–305.

Gähwiler BH, Capogna M, Debanne D, McKinney RA, Thompson SM (1997) Organotypic slice cultures: a technique has come of age. Trends Neurosci 20:471–477.

Gogolla N, Galimberti I, DePaola V, Caroni P (2006) Staining protocol for organotypic hippocampal slice cultures. Nat Protoc 1:2452–2456.

Gould E (1999) Serotonin and hippocampal neurogenesis. Neuropsychopharmacology 21:46S–51S.

Gross C, Zhuang X, Stark K, Ramboz S, Oosting R, Kirby L, Santarelli L, Beck S, Hen R (2002) Serotonin1A receptor acts during development to establish normal anxiety-like behaviour in the adult. Nature 416:396–400.

Gu JL, Müller S, Mancino V, Offermanns S, Simon MI (2002) Interaction of G alpha(12) with G alpha(13) and G alpha(q) signaling pathways. Proc Natl Acad Sci U S A 99:9352–9357.

Hayashi A, Nagaoka M, Yamada K, Ichitani Y, Miake Y, Okado N (1998) Maternal stress induces synaptic loss and developmental disabilities of offspring. Int J Dev Neurosci 16:209–216.

Herlenius E, Lagercrantz H (2001) Neurotransmitters and neuromodulators during early human development. Early Hum Dev 65:21–37.

Herzog A, Krell G, Michaelis B, Westerholz S, Helmke C, Braun K (2006) Geometrical modeling and visualization of pre- and post-synaptic structures in double-labeled confocal images. Paper presented at International Conference on Medical Information Visualization, July 2006, London, UK. (MediVis2006).

Hilaire G, Morin D, Lajard AM, Monteau R (1993) Changes in serotonin metabolism may elicit obstructive apnoea in the newborn rat. J Physiol 466:367–381.

Hoyer D, Hannon JP, Martin GR (2002) Molecular, pharmacological and functional diversity of 5-HT receptors. Pharmacol Biochem Behav 71:533–554.

Iftinca M, Hamid J, Chen L, Varela D, Tadayonnejad R, Altier C, Turner RW, Zamponi GW (2007) Regulation of T-type calcium channels by Rho-associated kinase. Nat Neurosci 10:854–860.

Ishiwata H, Shiga T, Okado N (2005) Selective serotonin reuptake inhibitor treatment of early postnatal mice reverses their prenatal stress-induced brain dysfunction. Neuroscience 133:893–901.

Iyengar R (1996) Gating by cyclic AMP: expanded role for an old signaling pathway. Science 271:461–463.

Jaffe AB, Hall A (2005) Rho GTPases: biochemistry and biology. Annu Rev Cell Dev Biol 21:247–269.

Jedlicka P, Papadopoulos T, Deller T, Betz H, Schwarzacher SW (2009) Increased network excitability and impaired induction of long-term potentiation in the dentate gyrus of collybistin-deficient mice in vivo. Mol Cell Neurosci 41:94–100.

Jeong SW, Ikeda SR (1999) Sequestration of G-protein beta gamma subunits by different G-protein alpha subunits blocks voltage-dependent modulation of Ca^{2+} channels in rat sympathetic neurons. J Neurosci 19:4755–4761.

Jontes JD, Smith SJ (2000) Filopodia, spines, and the generation of synaptic diversity. Neuron 27:11–14.

Katz LC, Shatz CJ (1996) Synaptic activity and the construction of cortical circuits. Science 274:1133–1138.

Kochlamazashvili G, Henneberger C, Bukalo O, Dvoretskova E, Senkov O, Lievens PM, Westenbroek R, Engel AK, Catterall WA, Rusakov DA, Schachner M, Dityatev A (2010) The extracellular matrix molecule hyaluronic acid regulates hippocampal synaptic plasticity by modulating postsynaptic L-type Ca(2+) channels. Neuron 67:116–128.

Korkotian E, Segal M (2001) Spike-associated fast contraction of dendritic spines in cultured hippocampal neurons. Neuron 30:751–758.

Kvachnina E, Liu G, Dityatev A, Renner U, Dumuis A, Richter DW, Dityateva G, Schachner M, Voyno-Yasenetskaya TA, Ponimaskin EG (2005) 5-HT7 receptor is coupled to G alpha subunits of heterotrimeric G12-protein to regulate gene transcription and neuronal morphology. J Neurosci 25:7821–7830.

Lauder JM (1990) Ontogeny of the serotonergic system in the rat: serotonin as a developmental signal. Ann N Y Acad Sci 600:297–313, discussion 314.

Lee T, Winter C, Marticke SS, Lee A, Luo L (2000) Essential roles of Drosophila RhoA in the regulation of neuroblast proliferation and dendritic but not axonal morphogenesis. Neuron 25:307–316.

Li Z, Van Aelst L, Cline HT (2000) Rho GTPases regulate distinct aspects of dendritic arbor growth in Xenopus central neurons in vivo. Nat Neurosci 3:217–225.

Lidov HG, Molliver ME (1982) Immunohistochemical study of the development of serotonergic neurons in the rat CNS. Brain Res Bull 9:559–604.

Lisman JE, Raghavachari S, Tsien RW (2007) The sequence of events that underlie quantal transmission at central glutamatergic synapses. Nat Rev Neurosci 8:597–609.

Lohmann C, Wong RO (2005) Regulation of dendritic growth and plasticity by local and global calcium dynamics. Cell Calcium 37:403–409.

Maletic-Savatic M, Malinow R, Svoboda K (1999) Rapid dendritic morphogenesis in CA1 hippocampal dendrites induced by synaptic activity. Science 283:1923–1927.

Manzke T, Dutschmann M, Schlaf G, Mörschel M, Koch UR, Ponimaskin E, Bidon O, Lalley PM, Richter DW (2009) Serotonin targets inhibitory synapses to induce modulation of network functions. Philos Trans R Soc Lond, B, Biol Sci 364:2589–2602.

Mattila PK, Lappalainen P (2008) Filopodia: molecular architecture and cellular functions. Nat Rev Mol Cell Biol 9:446–454.

Mazer C, Muneyyirci J, Taheny K, Raio N, Borella A, Whitaker-Azmitia P (1997) Serotonin depletion during synaptogenesis leads to decreased synaptic density and learning deficits in the adult rat: a possible model of neurodevelopmental disorders with cognitive deficits. Brain Res 760:68–73.

McEwen BS (1999) Stress and hippocampal plasticity. Annu Rev Neurosci 22:105–122.

Morita I, Kakuda S, Takeuchi Y, Kawasaki T, Oka S (2009) HNK-1 (human natural killer-1) glyco-epitope is essential for normal spine morphogenesis in developing hippocampal neurons. Neuroscience 164:1685–1694.

Müller M, Somjen GG (1998) Inhibition of major cationic inward currents prevents spreading depression-like hypoxic depolarization in rat hippocampal tissue slices. Brain Res 812:1–13.

Narita N, Narita M, Takashima S, Nakayama M, Nagai T, Okado N (2001) Serotonin transporter gene variation is a risk factor for sudden infant death syndrome in the Japanese population. Pediatrics 107:690–692.

Naughton M, Mulrooney JB, Leonard BE (2000) A review of the role of serotonin receptors in psychiatric disorders. Hum Psychopharmacol 15:397–415.

Newey SE, Velamoor V, Govek EE, Van Aelst L (2005) Rho GTPases, dendritic structure, and mental retardation. J Neurobiol 64:58–74.

Oertner TG, Matus A (2005) Calcium regulation of actin dynamics in dendritic spines. Cell Calcium 37:477–482.

Oertner TG, Sabatini BL, Nimchinsky EA, Svoboda K (2002) Facilitation at single synapses probed with optical quantal analysis. Nat Neurosci 5:657–664.

Okado N, Cheng L, Tanatsugu Y, Hamada S, Hamaguchi K (1993) Synaptic loss following removal of serotoninergic fibers in newly hatched and adult chickens. J Neurobiol 24:687–698.

Olson NC (1987) Role of 5-hydroxytryptamine in endotoxin-induced respiratory failure of pigs. Am Rev Respir Dis 135:93–99.

Ponimaskin E, Voyno-Yasenetskaya T, Richter DW, Schachner M, Dityatev A (2007) Morphogenic signaling in neurons via neurotransmitter receptors and small GTPases. Mol Neurobiol 35:278–287.

Ponimaskin EG, Profirovic J, Vaiskunaite R, Richter DW, Voyno-Yasenetskaya TA (2002) 5-Hydroxytryptamine 4(a) receptor is coupled to the Galpha subunit of heterotrimeric G13 protein. J Biol Chem 277:20812–20819.

Pugliese AM, Passani MB, Corradetti R (1998) Effect of the selective 5-HT1A receptor antagonist WAY 100635 on the inhibition of e.p.s.ps produced by 5-HT in the CA1 region of rat hippocampal slices. Br J Pharmacol 124:93–100.

Rusakov DA, Fine A (2003) Extracellular Ca^{2+} depletion contributes to fast activity-dependent modulation of synaptic transmission in the brain. Neuron 37:287–297.

Saghatelyan AK, Dityatev A, Schmidt S, Schuster T, Bartsch U, Schachner M (2001) Reduced perisomatic inhibition, increased excitatory transmission, and impaired long-term potentiation in mice deficient for the extracellular matrix glycoprotein tenascin-R. Mol Cell Neurosci 17:226–240.

Saito Y, Ito M, Ozawa Y, Obonai T, Kobayashi Y, Washizawa K, Ohsone Y, Takami T, Oku K, Takashima S (1999) Changes of neurotransmitters in the brainstem of patients with respiratory-pattern disorders during childhood. Neuropediatrics 30:133–140.

Scott R, Lalic T, Kullmann DM, Capogna M, Rusakov DA (2008) Target-cell specificity of kainate autoreceptor and Ca2+-store-dependent short-term plasticity at hippocampal mossy fiber synapses. J Neurosci 28:13139–13149.

Semenova MM, Mäki-Hokkonen AMJ, Cao J, Komarovski V, Forsberg KM, Koistinaho M, Coffey ET, Courtney MJ (2007) Rho mediates calcium-dependent activation of p38alpha and subsequent excitotoxic cell death. Nat Neurosci 10:436–443.

Stoppini L, Buchs PA, Muller D (1991) A simple method for organotypic cultures of nervous tissue. J Neurosci Methods 37:173–182.

Tata DA, Anderson BJ (2010) The effects of chronic glucocorticoid exposure on dendritic length, synapse numbers and glial volume in animal models: implications for hippocampal volume reductions in depression. Physiol Behav 99:186–193.

Thomas DR, Melotto S, Massagrande M, Gribble AD, Jeffrey P, Stevens AJ, Deeks NJ, Eddershaw PJ, Fenwick SH, Riley G, Stean T, Scott CM, Hill MJ, Middlemiss DN, Hagan JJ, Price GW, Forbes IT (2003) SB-656104-A, a novel selective 5-HT7 receptor antagonist, modulates REM sleep in rats. Br J Pharmacol 139:705–714.

Turrigiano GG (2008) The self-tuning neuron: synaptic scaling of excitatory synapses. Cell 135:422–435.

Udo H, Jin I, Kim JH, Li HL, Youn T, Hawkins RD, Kandel ER, Bailey CH (2005) Serotonin-induced regulation of the actin network for learning-related synaptic growth requires Cdc42, N-WASP, and PAK in Aplysia sensory neurons. Neuron 45:887–901.

Vanhoenacker P, Haegeman G, Leysen JE (2000) 5-HT7 receptors: current knowledge and future prospects. Trends Pharmacol Sci 21:70–77.

Whitaker-Azmitia PM (2005) Behavioral and cellular consequences of increasing serotonergic activity during brain development: a role in autism? Int J Dev Neurosci 23:75–83.

Woehler A, Ponimaskin EG (2009) G protein–mediated signaling: same receptor, multiple effectors. Curr Mol Pharmacol 2:237–248.

Wood M, Chaubey M, Atkinson P, Thomas DR (2000) Antagonist activity of meta-chlorophenylpiperazine and partial agonist activity of 8-OH-DPAT at the 5-HT(7) receptor. Eur J Pharmacol 396:1–8.

Yan W, Wilson CC, Haring JH (1997) 5-HT1a receptors mediate the neurotrophic effect of serotonin on developing dentate granule cells. Brain Res Dev Brain Res 98:185–190.

Yu JZ, Dave RH, Allen JA, Sarma T, Rasenick MM (2009) Cytosolic G{α}s acts as an intracellular messenger to increase microtubule dynamics and promote neurite outgrowth. J Biol Chem 284:10462–10472.

Zheng JQ, Poo MM (2007) Calcium signaling in neuronal motility. Annu Rev Cell Dev Biol 23:375–404.